ornl

OAK
RIDGE
NATIONAL
LABORATORY

UNION
CARBIDE

OPERATED BY
UNION CARBIDE CORPORATION
FOR THE UNITED STATES
DEPARTMENT OF ENERGY

NUREG/CR-2811
ORNL-5895

Development of Techniques for Fabrication of Film Probe Sensor Assembly

A. J. Moorhead

Prepared for the
U.S. Nuclear Regulatory Commission
Office of Nuclear Regulatory Research
Under Interagency Agreement DOE 40-551-75

Printed in the United States of America. Available from
National Technical Information Service
U.S. Department of Commerce
5285 Port Royal Road, Springfield, Virginia 22161

Available from

GPO Sales Program
Division of Technical Information and Document Control
U.S. Nuclear Regulatory Commission
Washington, D.C. 20555

NUREG/CR-2811
ORNL-5895
Dist. Category R5

METALS AND CERAMICS DIVISION

DEVELOPMENT OF TECHNIQUES FOR FABRICATION OF FILM PROBE SENSOR ASSEMBLY

A. J. Moorhead

Manuscript Completed - September 10, 1982

Date Published - October 1982

Notice: This document contains information of a preliminary nature. It is subject to revision or correction and therefore does not represent a final report.

Prepared for the
U.S. Nuclear Regulatory Commission
Office of Nuclear Regulatory Research
Washington, D.C. 20555
Under Interagency Agreement DOE 40-551-75

NRC FIN No. B0413

Prepared by the
OAK RIDGE NATIONAL LABORATORY
Oak Ridge, Tennessee 37830
operated by
UNION CARBIDE CORPORATION
for the
U.S. DEPARTMENT OF ENERGY

Under Contract No. W-7405-eng-26

CONTENTS

DEVELOPMENT OF TECHNIQUES FOR FABRICATION OF FILM PROBE SENSOR ASSEMBLY

A. J. Moorhead

ABSTRACT

Pulsed laser welding and brazing techniques were developed for fabrication of sensors designed to measure liquid film properties in out-of-reactor safety tests that simulate a loss-of-coolant accident in a pressurized-water nuclear reactor. These sensors were made possible by a unique ceramic-to-metal seal system based on a cermet insulator and a brazing filler metal, both developed at ORNL. This seal system was shown to resist steam to an exposure of at least 100 h at 700°C (1292°F) and to resist repetitive thermal transients of 300°C/s (540°F). The film property sensors described differ from our earlier work in that (1) the sensor subassembly body contains larger electrodes and consequently a larger cermet insulator and (2) the triaxial instrumentation cables, which also contain a high-temperature ceramic-to-metal seal, are only 1.60 mm (0.063 in.) in diameter rather than the 3.18-mm (0.125-in.) diameter used previously. Thus, this report describes the successful adaptation of the previously developed ceramic-to-metal seal system to a sensor subassembly containing both significantly larger and smaller brazed components. Procedures were also developed for induction brazing the instrumentation cables to a stainless steel end cap and for laser welding this component to the brazed sensor body itself. Cable end seals and sensor bodies fabricated with these designs and techniques maintained excellent helium leaktightness ($<3 \times 10^{-6}$ cm^3/s) after 20 severe thermal shock tests from 500°C air into water at 80°C.

INTRODUCTION

A joint program to study three-dimensional two-phase (steam-water) fluid flow phenomena in the upper plenum and core of a pressurized-water nuclear reactor during the reflood stage of a loss-of-coolant accident (LOCA) was undertaken by the U.S. Nuclear Regulatory Commission in cooperation with its counterparts in West Germany and Japan. The overall objectives of the program were to determine

1. whether steam that is formed inside a reactor core during a postulated LOCA can block the movement of emergency coolant into the core,

2. how the emergency coolant redistributes itself horizontally and vertically as it moves through the heated core, and
3. how the steam and water move and interact in the core downcomer and upper portion of the reactor while the coolant water fills the lower part of the reactor and starts to cool the core.

The role of ORNL under the Advanced Instrumentation for Reflood Studies (AIRS) Program was to develop and supply instrumentation systems for measurement of flow parameters such as void fraction, fluid velocity, and film thickness in large simulated segments of core assemblies that use electrically heated fuel rod simulators instead of radioactive fuel pins. In the portion of a LOCA to be studied in the Primärkreislauf (PKL) facility in Germany and the Slab Core Test Facility (SCTF) in Japan, known as reflood, the general thermal cycle that film probe sensors will experience is a rise in temperature to about 700°C over a period of about 10 min, followed by a rapid decrease in temperature with a transient of up to about 300°C/s. The pressure to which the sensors will be exposed, at least in some tests, will be 0.7 MPa, gage (100 psig). This cycle would occur in a reactor core after loss of coolant; the temperature rises and then sharply decreases when coolant is introduced from the emergency core cooling system. A more complete description of the typical test cycle in the PKL facility was given previously[1] along with a discussion of the invention of the metal-dispersion-enhanced alumina insulator by C. S. Morgan and our development of materials and techniques for fabricating impedance probes that measure fluid velocity and direction of flow in high-temperature steam and water mixtures. The thermal cycle in the SCTF was considered equal to that of PKL for the purposes of our fabrication development work.

SENSOR GEOMETRY

The electrode geometry of the two types of film probe sensors and their arrangement within a sensor module for the SCTF-I wall or upper plenum assembly is shown in Fig. 1. Although some aspects of the design of the probes for PKL-II are different from those for SCTF-I (e.g., body size and module geometry), the essential geometry is the same, and the designs will be treated as one in this report. Note that three of the sensors have electrodes with a *D* geometry, whereas the electrodes are essentially trapezoids in the fourth sensor. Two of the *D*-electrode sensors are excited with a 2-V rms signal at 2 kHz to measure the film thickness during a reflood test. The sensors can measure films with a minimum thickness of about 0.1 mm. By correlation of the signal between the two film thickness sensors, the velocity of a wave passing through the film can be determined. The sensor with the trapezoidal electrodes is excited by a 100-kV dc signal and responds to both film thickness and velocity. By cross-correlation with one of the film thickness sensors, the component of the signal attributable to only fluid velocity can be extracted. Unfortunately this electrolysis potential (EP) probe is also very sensitive to the conductivity of water. Therefore, the fourth

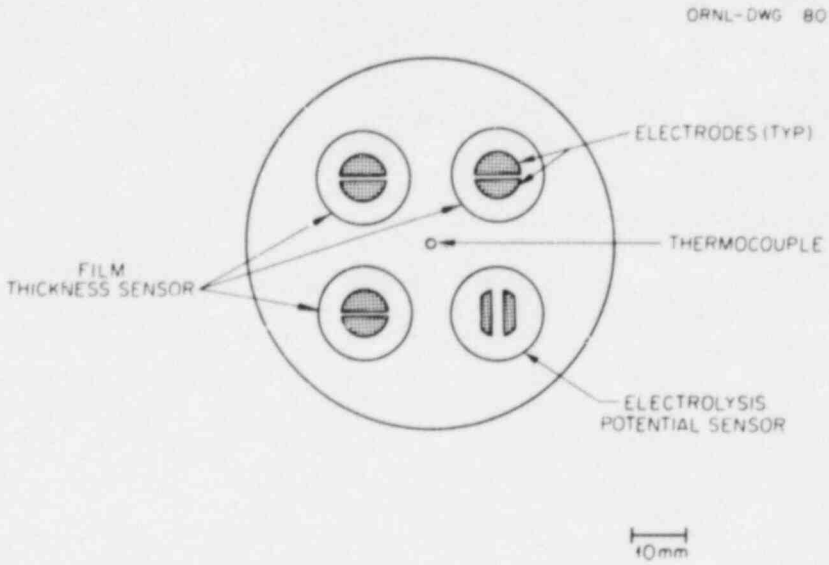

Fig. 1. Configuration of Slab Core Test Facility-I wall and upper plenum film probe assembly.

sensor in the module is excited with a 10-V rms signal at 100 kHz to measure conductivity of the water at that particular location to correct the signal from the EP probe. The electronic signals are carried to and from each electrode by small-diameter, stainless-steel-sheathed cables. Each cable is protected from moisture penetration by a brazed ceramic-to-metal seal on the sensor end. Much more complete explanations of the theory of the electrode geometry, sensor operation and calibration, and development of the appropriate instrumentation are presented elsewhere.[2,3]

CABLE END SEAL DEVELOPMENT

FABRICATION

Although many of the problems of developing a seal for the 1.60-mm-diam triaxial stainless steel cable had been solved previously in our work on the end seal for the 3.18-mm-diam cable,[1] the effort reported here was still challenging because of the small size of the new cable and its seal. We first considered a simple scale-down of the seal of the larger cable, which had a platinum transition sleeve with the same outside diameter as that of the outer sheath of the cable and a tapered braze joint between the sleeve and the outer sheath. The purpose of the platinum transition joint is to accommodate the large difference in thermal expansion of the cermet and that of the type 304 stainless steel cable. However, we soon realized that machining the female portion of the tapered joint on the inside of the 1.60-mm-diam cable would be much more difficult than on the 3.18-mm-diam cable. Also, the cermet insulator required for such a design (the same diameter as the inner

diameter of the outer sheath) would be only 1.07 mm (0.042 in.) in diameter with a required length of about 5 mm — a difficult length-to-diameter ratio for grinding. The latter concern was compounded when our machinists had little success in boring a 0.28-mm-diam (0.011-in.) hole through 5-mm-thick platinized alumina insulator test blanks. We were therefore forced again to use 0.51-mm-diam (0.020-in.) platinum wire for the central lead extension because we were successful in drilling a hole through the cermet to accommodate this size. Thus, if we had used a scaled-down version of our 3.18-mm cable end seal, we would have had a 0.53-mm-diam (0.021-in.) hole bored through an insulator having a diameter of only 1.07 mm (0.042 in.), leaving the wall too thin and the insulation path too short. We therefore experimented with the oversleeve design shown in Fig. 2 and, because of our early and consistent success with brazed end seals of this geometry, have relied on this design with only a few minor dimensional changes. Note that the platinum transition of this new design is greater in diameter than the cable, whereas in the design for the 3.18-mm-diam cable it was the same size. However, this local perturbation in geometry is easily accommodated and has not caused the space problems that the larger cable caused when it was used in our guide tube impedance probes fabricated for the PKL system in Germany. Therefore, we also used the 1.60-mm-diam cable in the guide tube probes recently shipped to Japan for installation in the SCTF.

Two methods were used for attaching the 0.51-mm-diam (0.020-in.) platinum extension wire to the 0.28-mm-diam (0.011-in.) type 304 stainless steel central conductor wire of the triaxial cable: laser welding and brazing. The purpose of the transition to platinum wire is to use

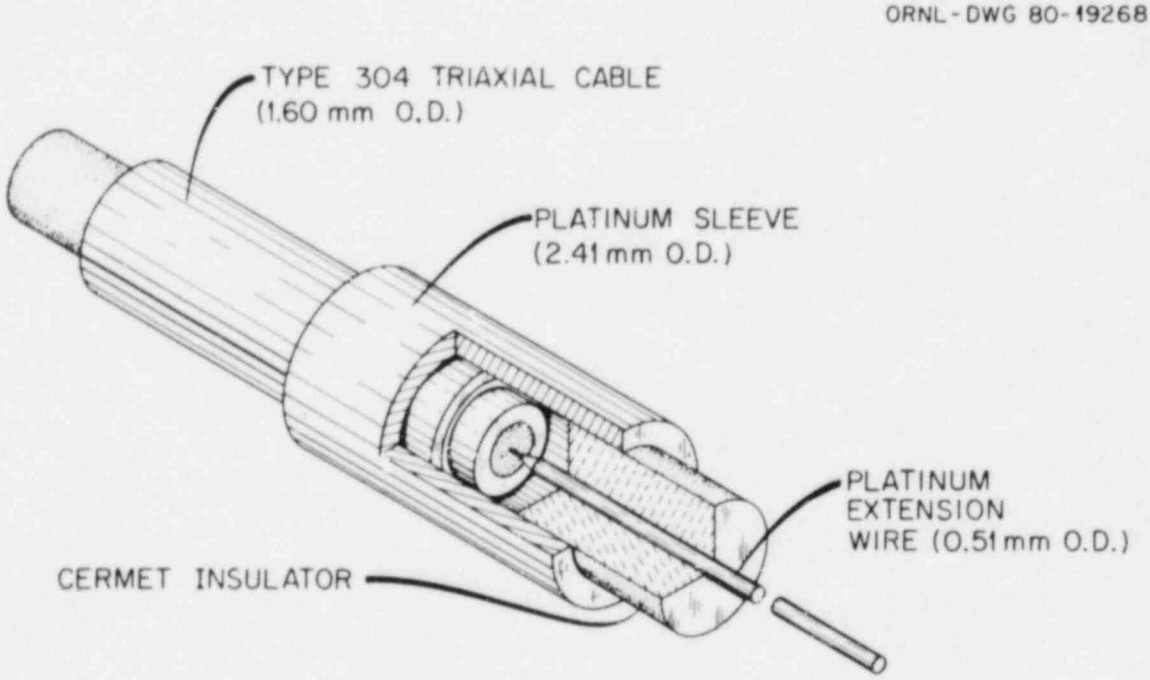

Fig. 2. Design of brazed end seal for 1.60-mm-diam (0.063-in.) type 304 stainless steel triaxial cable.

this ductile lower thermal expansion material in contact with the low thermal expansion alumina cermet to minimize thermal expansion mismatch problems on cooldown from brazing.

On most cables fabricated to date, the wires were joined by pulsed ruby laser welding with the fixture shown in Fig. 3. Four pulses were used for each weld with the center of the spot shifted to the platinum side of the joint. A 94.8-mm focal-length lens with an energy output of 10 J per pulse was used. To match the diameters of the two wires, the platinum wire was tapered on the end by sanding with emery paper. We found that, unless the cable end was annealed at 1050°C before attaching the extension wire, failure of the laser weld was likely during assembly of the cermet and transition sleeve for brazing. Such

Y-173500

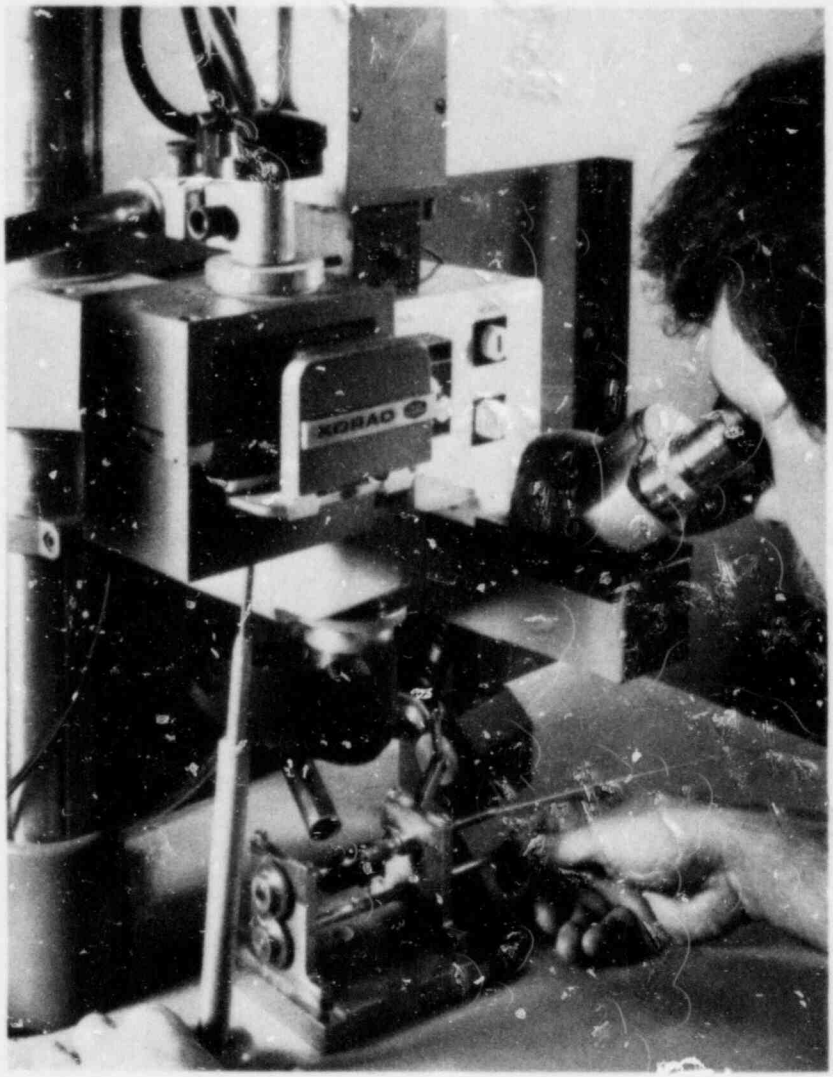

Fig. 3. Laser welding of type 304 stainless steel central conductor to platinum extension wire.

failures apparently result from the stiffness of the cold-worked central conductor wire and/or contamination on the wire surface. Vacuum annealing also removed any moisture that might have penetrated the cable during end preparation so that the electrical loss factor of the cable was returned to an acceptable level of less than 0.010.

We developed a brazing technique as an alternative to laser welding for attachment of the platinum extension wire for the following purposes:

1. as a potential means of increasing cable production,
2. as a response to concerns about weld quality after metallographic examination of some of the laser welds, and
3. as a means for subcontractors not having a laser welder to seal cables.

Joint preparation for brazing consisted of drilling a 0.33- to 0.36-mm-diam by 1.60-mm-deep (0.013- to 0.014- by 0.063-in.) hole in one end of the 75-mm-long (3-in.) platinum wire so that the central conductor wire of the triaxial cable could be inserted. The brazing filler metal was AWS A5.8, class BAu-4 (82% Au-18% Ni), powder mixed with an acrylic binder. Brazing was in a vacuum tube furnace for 60 s at 980°C as determined by a 1.60-mm-diam sheath-type thermocouple adjacent to the five cables brazed in a batch. Samples of lead extensions attached by each technique are shown in Fig. 4.

Brazing does not add another heating cycle to our fabrication process because the brazing operation is performed in lieu of the normal thermal treatment of all cables to remove moisture and other contaminants before attaching the end seal components. In the case of brazing rather than laser welding the central wire extension, the thermal cycle goes to 980°C rather than to 1050°C (also used to anneal the central wire for laser welding), but we have observed no deterioration in the quality of the subsequent brazed end seals from this lower temperature treatment.

A series of five each of laser-welded and brazed lead extensions was tensile tested at room temperature to gage their respective strengths. Because we would expect a low load to bring about failure in the 0.51-mm-diam (0.020-in.) platinum wire, we used a series of balance weights hung on the wire rather than a testing machine to determine the strength of the joints. The results of these tests are given in Table 1. The average data strongly favor the brazing technique. However, if the data from sample 1 are discarded (because of anomalous failure within the stainless steel wire at a much lower load than the expected 25 kg), the average failure load of the four remaining laser welds is 2.50 kg, which compares well with the 2.58-kg average of the brazements. The joint fit-up or brazing cycle could likely be altered slightly so that failure could be made to occur outside the joint area in the platinum wire. However, because the joint is stressed primarily by loads involved with end seal assembly before brazing, we think the present design is more than adequate. Thus, either of the two techniques is acceptable. Typical photomicrographs of each type of joint are shown in Fig. 5.

After the lead was attached, the components were assembled for end seal brazing as shown in Fig. 6. The active-metal direct-brazing

ORNL-PHOTO 5451-80

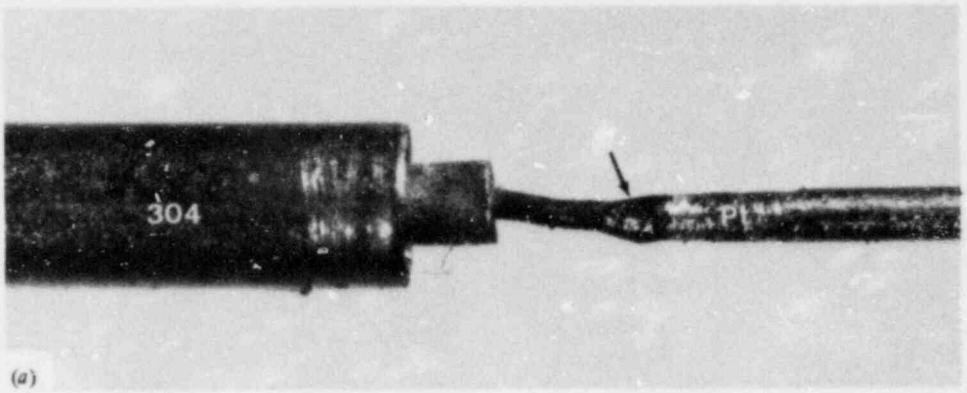

(*a*)

ORNL-PHOTO 5456-80

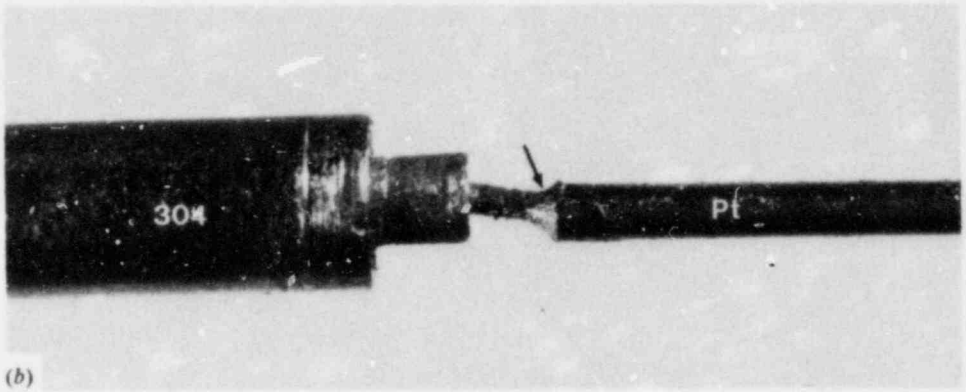

(*b*)

Fig. 4. Examples of two techniques for connecting central conductor of 1.60-mm-diam triaxial cable and 0.51-mm-diam platinum extension wire. The joint area in each case is indicated by an arrow. (*a*) Laser weld. (*b*) Furnace braze.

filler was 49% Ti–49% Cu–2% Be. The alloy was applied as −100-mesh powder mixed in an acrylic binder. The powder was produced by crushing a 25-g arc-melted button in a steel mortar and pestle. A permanent magnet was drawn repetitively through the crushed and seived powder to remove any steel particles. The cable end seals were brazed in batches of five in a resistance-heated ceramic tube vacuum furnace (Fig. 7).

We found that both the leaktightness of the ceramic-to-metal seal brazement and its resistance to thermal shock were greatly enhanced by high-temperature oxidation treatment of the platinized alumina insulators. This cycle consists of heating in air from room temperature to 1500°C for about 15 min, holding at temperature for 120 s, and cooling back to room temperature in about 30 min. Whether this treatment is effective because it removes contaminants (such as machining coolant) from the cermet or because the stoichiometry of the insulator is changed is unknown, but it has greatly improved the quality of our end seal brazements.

Table 1. Room-temperature strength of laser-welded and brazed joints between the 0.27-mm-diam type 304 stainless steel central conductor and 0.51-mm-diam platinum extension wire

Sample	Load to failure[a]		Stress in Pt at failure[a]		Location of failure
	(kg)	(lb)	(MPa)	(ksi)	
			Laser-welded joint[b]		
1	0.70	1.54	33.9	4.9	Stainless steel wire just outside weld
2	3.20	7.05	154.8	22.5	Within the weld
3	1.50	3.31	72.6	10.5	Within the weld
4	2.00	4.41	96.8	14.0	Within the weld
5	3.30	7.28	159.7	23.2	Within the weld
Av	2.14	4.72	103.6	15.0	
			Furnace-brazed joint[c]		
6	2.30	5.07	111.3	16.1	Within the Pt wire at the base of drilled hole
7	2.50	5.51	121.0	17.5	Within the Pt wire at the base of drilled hole
8	3.20	7.05	154.8	22.5	Within the Pt wire at the base of drilled hole
9	2.40	5.29	116.1	16.8	Within the Pt wire at the base of drilled hole
10	2.50	5.51	121.0	17.5	Within the Pt wire at the base of drilled hole
Av	2.58	5.69	124.8	18.1	

[a] Average load to failure of four samples of type 304 stainless steel base metal was 4.95 kg, ultimate tensile strength of 751.6 MPa (109 ksi); average load to failure of unjoined platinum wire was 4.1 kg, ultimate tensile strength of 206.5 MPa (30 ksi).

[b] Four 10-J pulses from a ruby laser welder.

[c] Brazed with 82% Au-18% Ni filler metal in a vacuum for 60 s at 980°C.

Y-177462

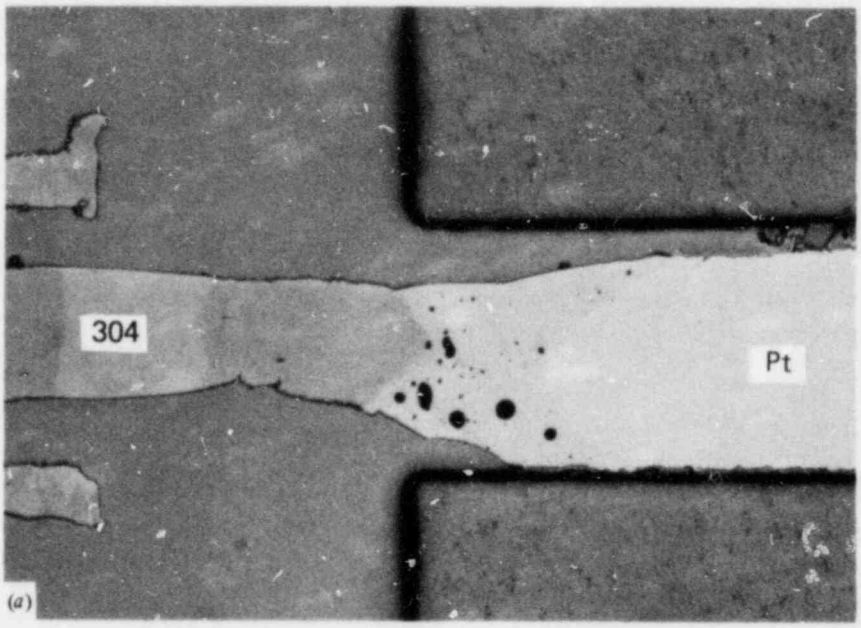

400 μm

Y-175055

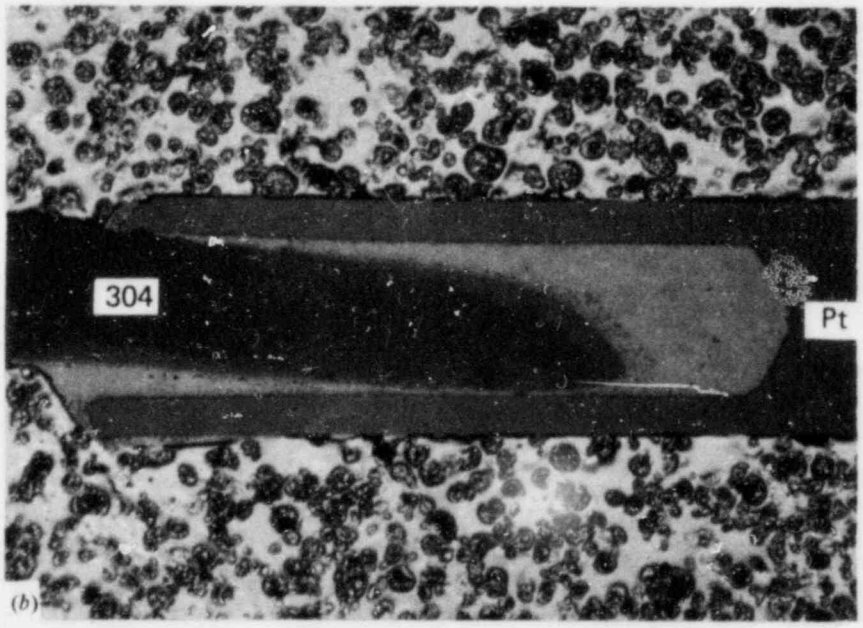

Fig. 5. Microstructure of two types of joints between 0.38-mm-diam type 304 stainless steel central conductor and 0.51-mm-diam platinum extension wire. (*a*) Pulse laser welded. (*b*) Vacuum furnace brazed with 82% Au-18% Ni.

ORNL-PHOTO 4153-80

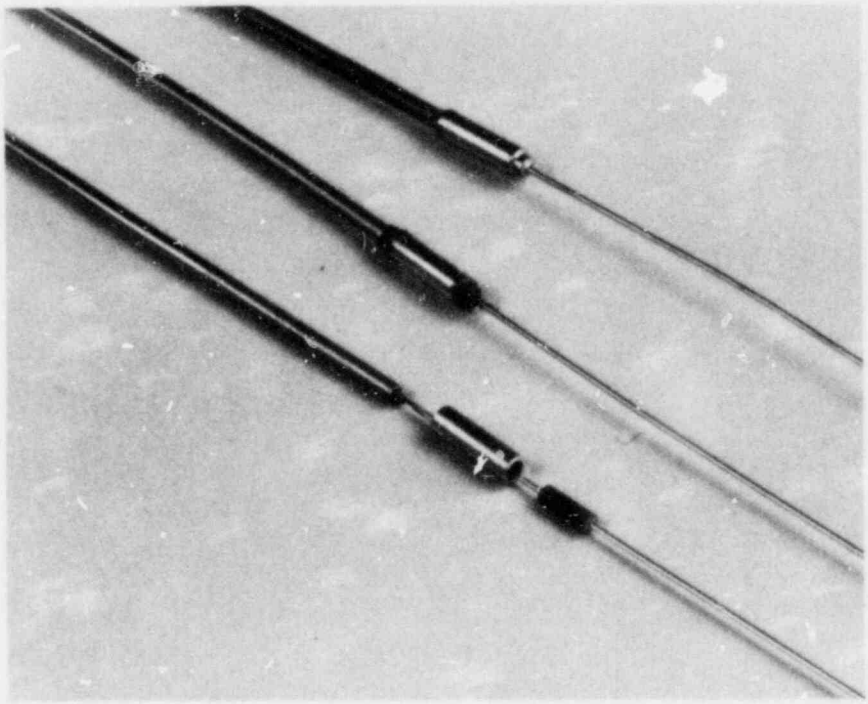

Fig. 6. Assembly steps for end seal on 1.60-mm-diam triaxial cable. Bottom, platinum sleeve and cermet insulator on the cable. Center, after application of brazing filler metal powder. Top, after brazing.

During brazing, an electrically conductive path typic[illegible] cross the cermet insulator from the center lead extension to the pl[illegible] transition sleeve as the result of the extreme fluidity of th[illegible]e filler metal. External shorts of this nature are readily cleared by abrading the edge of the insulator with an abrasive stone to remove any metallic film, and electrical resistances between any two of the three conductors in a cable are typically 10^5 to 10^6 Ω. Data from a random sampling of cables that were assembled into in-wall film sensors for SCTF are given in Table 2. The electrical loss factor after brazing for these cables averaged 0.218, significantly greater than the maximum acceptable value of 0.010.

Heat-shrinkable tubing had been applied to both ends of these cables immediately after machining the ends for brazing. However, we believe that the degradation in electrical properties is caused both by moisture that bypasses the tubing and by an electrically conductive film produced during brazing. We hypothesize that this film is a combination of condensed metallic vapors from the molten brazing filler metal and a carbonaceous residue left from the decomposition of the commercial plastic binder used to hold the braze alloy powder in place. Any tendencies for producing a conductive film or residue are compounded by the close confines of the small cavity within the cable end seal.

ORNL-PHOTO 4148-80

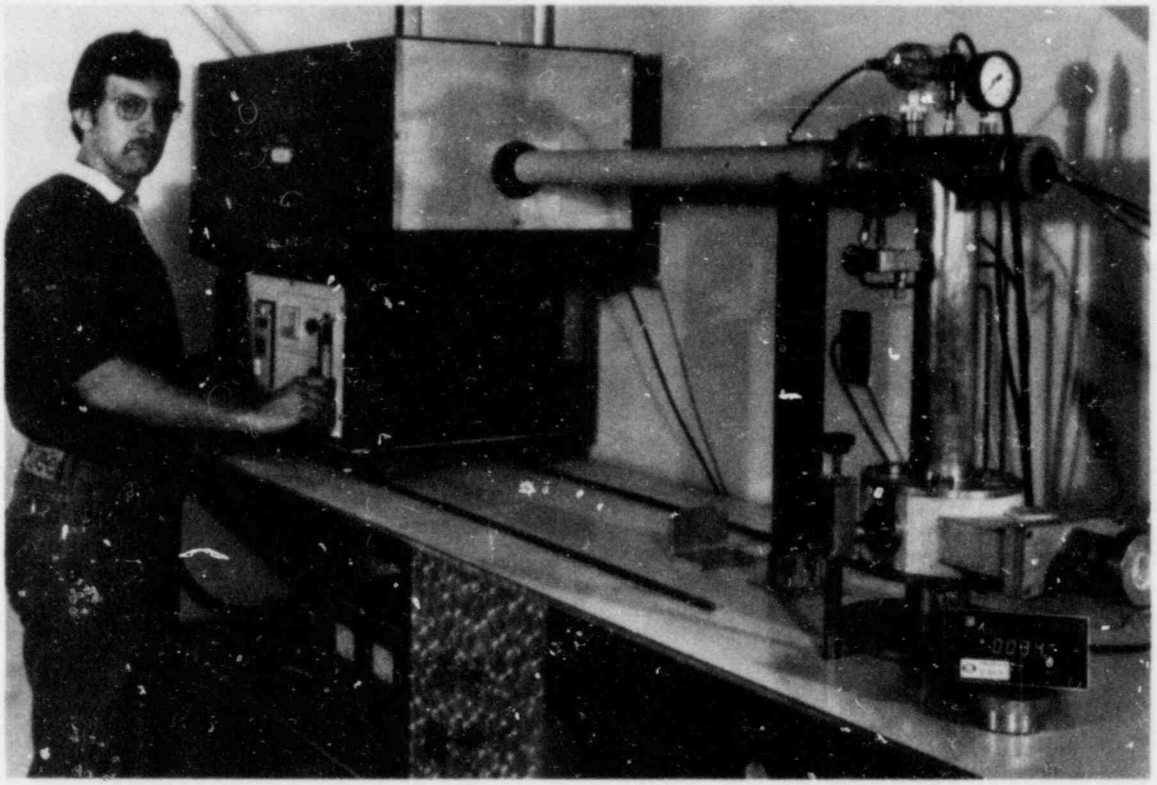

Fig. 7. Vacuum furnace with movable heating element being used to braze end seals on a batch of triaxial cables.

Although the filler metal binder is purported to leave no residue on heating above 315°C (600°F), we found in careful tests that a very light conductive deposit was left after heating in vacuum to our cable end seal-brazing temperature of 930°C. Although the resistance of this film, measured over distances of about 1 mm, was in general greater than 10^6 Ω, we sometimes found residues with resistances of about 10^5 Ω. In one instance residues from two identical binder samples (from the same lot of material) had significantly different resistances. However, close examination revealed one sample to be from an almost-empty can. Over a long period of use, the solvent in that container likely evaporated and left a binder that was more highly concentrated in the plastic material, which produced a more conductive residue film on heating. This concentration of plastic in the slurry of braze alloy powder and binder can also occur with repeated use of the same container of alloy if care is not taken to remove the binder from the powder after application to each batch of cables. We routinely do this by repeated acetone washings of the slurry.

No matter what mechanism causes degradation of the cable electrical properties during end seal fabrication, we found two techniques that proved highly beneficial in restoring the resistance and loss of the cables to their original values. The first technique consists of heating

Table 2. Helium leak rate and electrical properties of some of the 1.60-mm-diam by 9.45-m-long triaxial cables with brazed end seals assembled in the in-wall film sensors for Slab Core Test Facility

Cable	Helium leak rate[a] (cm^3/s)	Resistance[b]		Capacitance[b]		Loss	
		As brazed (Ω)	After bakeout[c] (Ω)	As brazed (nF)	After bakeout[c] (nF)	As brazed	After bakeout[c]
150	2.0×10^{-10}	7.5×10^{6}	6.5×10^{7}	4.37	4.34	0.099	0.002
151	1.6×10^{-7}	5.7×10^{6}	2.7×10^{8}	4.21	4.18	0.042	0.002
152	1.0×10^{-10}	6.0×10^{6}	5.5×10^{7}	4.26	4.23	0.033	0.002
153	5.0×10^{-9}	4.0×10^{6}	3.0×10^{8}	4.17	4.07	0.134	0.001
172	2.9×10^{-9}	6.0×10^{5}		4.44	4.08	0.199	0.010
173	1.0×10^{-9}	1.5×10^{5}	1.4×10^{9}	4.22	4.03	0.056	0.001
175	9.0×10^{-10}	7.0×10^{6}	1.4×10^{10}	4.31	4.21	0.038	0.001
176	7.8×10^{-10}	6.5×10^{6}	1.6×10^{8}	4.24	4.09	0.044	0.001
186	8.0×10^{-10}	6.7×10^{5}	6.5×10^{9}	4.24	4.06	0.491	0.002
187	8.3×10^{-10}	9.0×10^{5}	1.6×10^{9}	4.13	4.01	0.308	0.001
188	8.6×10^{-10}	3.7×10^{10}	9.5×10^{9}	4.20	4.02	0.287	0.001
189	7.6×10^{-10}	2.5×10^{6}		4.38	4.16	0.132	0.001
243	1.0×10^{-9}	1.2×10^{6}	1.7×10^{9}	4.28	4.16	0.565	0.002
244	1.2×10^{-9}	3.0×10^{6}	6.0×10^{8}	4.13	4.06	0.346	0.001
235	1.8×10^{-9}	7.0×10^{5}	1.1×10^{9}	4.30	3.63	0.566	0.001
246	5.0×10^{-10}	1.5×10^{6}	1.1×10^{10}	4.14	4.06	0.254	0.001

[a]Ceramic-to-metal seal area on cable end, pressurized for 10 min with helium at 0.6 MPa, gage (80 psig) and inserted into a fitting connected to a mass spectrometer leak detector.

[b]Measured between central conductor wire and inner sheath.

[c]Held a minimum of 24 h at 350°C in vacuum of about 0.1 MPa (29 in. Hg) with liquid nitrogen cold trap to assist in moisture removal.

batches of brazed cable (with heat-shrinkable tubing removed from the instrument end) for at least 24 h in a low vacuum at 350°C. This was accomplished in a long stainless steel pipe connected to a mechanical roughing pump and wrapped externally with tubular heating elements and insulation. After this vacuum bakeout treatment, most cables had acceptably high resistance and losses of less than the maximum permitted 0.010 as shown by the after-bakeout data in Table 2.

The second treatment, consisting of heating the end seal area in air at 450°C for 15 min, was given to cables whose properties were insufficiently improved by the vacuum bakeout. This was performed by inserting the cables through an opening in the door of a small box furnace so that only the end seal and about 150 mm (6 in.) of the cable were heated. This treatment caused only slight oxidation of the brazing filler metal and cable but many times was sufficient to improve cable electrical properties. This improvement evidently was the result of oxidation of the conductive film responsible for the unacceptable properties (generally too high a loss factor).

TESTING

The most stringent requirement of the cable end seals is the maintenance of adequate leaktightness after exposure to high-temperature steam and water and repeated severe thermal transients. Although the purpose of the leaktightness requirement is to exclude moisture from inside the cable, all our tests were based on helium permeability because it is a more easily measured property. The degradation of cable electrical properties does not seem to result from the presence of water per se but from interaction of the water with the aluminum oxide insulation to form, in effect, an electrolytic capacitor. Tests by the instrument and sensor designers showed the system to be relatively intolerant to moisture in the cables. Rough calculations indicate that a cable can still function if the steam leakage rate corresponding to a room-temperature helium leak rate of about 10^{-3} cm^3/s is not exceeded over the period of testing. Because of uncertainties in these calculations and the expected increase in end seal leakage under extended service conditions, we selected 4×10^{-7} cm^3/s as the maximum permissible helium leak rate for a cable end seal when the cable is installed in a sensor subassembly. This is actually a very conservative number because the cable end seals are not actually exposed to the test environment itself but are enclosed within the sensor body, which is also helium leaktight by virtue of its various weld and braze joints.

Temperature data provided by the Germans and Japanese indicated that these sensors would be exposed to short thermal transients of about 300°C/s during each reflood test cycle. Instrumented quench tests indicated that small parts that were dropped from an open tube furnace at 500°C into a container of water at 80°C cooled at rates considerably in excess of 300°C/s. The ability to withstand this quench test was therefore taken as one criterion for all ceramic-to-metal seal designs. This requirement was also taken for the cable end seals although the thermal transient on an end seal isolated from the reflood cooling water by the subassembly housing would apparently be much less severe.

Shown in Table 3 are typical helium leak rates for five short lengths of cable. The cables had been sealed on one end with a platinum oversleeve, an insulator of alumina containing dispersed platinum, and a platinum central lead extension and then had been quenched from air at 500°C into water at 80°C. Photomicrographs of cable 3 in the table are shown in Fig. 8. The brazing filler metal was 49% Ti–49% Cu–2% Be, and the brazing temperature was 930°C with no hold time at temperature. The leak rates were measured by inserting the open end of the cable into a mass spectrometer leak detector and flowing helium over the end seal area. Short lengths of cables were used for these quench tests to facilitate quenching. We found that the cable insulation is sufficiently permeable to helium to give a valid leak check if the length of cable is about 50 mm.

The end seals on the long lengths of cables [up to 9.5 m (31 ft)] to be attached to the film property sensors are leak checked by pressurizing the external seal area for 10 min with helium at 0.6 MPa, gage (80 psig), removing pressure, and quickly inserting into the port of the leak detector. Table 3 also contains seal leak data taken by this method for two long cables that were tested by heating in a wet helium atmosphere to 300°C and quenching with a water spray.

A similar test was given each cable immediately after brazing, but the seal was pressurized for only 1 min with helium at 0.3 MPa, gage (50 psig) and then immersed in alcohol and observed for bubble formation rather than being connected to the leak detector. This rapid test, which can detect leaks of about 10^{-6} cm^3/s, was used for rapid identification of cable seals in need of rebrazing. The lower pressure and shorter time were used to minimize the amount of helium that would be forced into the cable if it had a leak. This trapped gas causes problems in rebrazing a cable by tending to flow out through the molten alloy, thus preventing a leaktight seal. Therefore, end seals to be rebrazed were routinely heated for 30 min at 600°C in vacuum to ensure that the helium pressure inside the seal cavity was reduced to an acceptable level.

SENSOR SUBASSEMBLY DEVELOPMENT

The design of the SCTF-I in-wall film sensor subassembly is shown in Fig. 9. The choice of materials and their geometric arrangement were based on the need for accommodating the relatively low thermal expansion of the cermet insulator (6.5×10^{-6}/°C) in an oxidation-resistant metallic body having a higher thermal expansion. As in our earlier work, this accommodation was accomplished with a platinum transition ring between the insulator and body, platinum having a coefficient of thermal expansion above that of the cermet but below that of stainless steels. To further reduce the thermal expansion mismatch, we used ferritic type 446 stainless steel in the sensor body rather than the more common austenitic type 304. Type 446 stainless steel has a mean coefficient of thermal expansion (0–1000°C) of 13.7×10^{-6}/°C compared with 20.2×10^{-6}/°C for type 304 (ref. 4).

The components for an in-wall film probe subassembly for the PKL reflood facility are shown in Fig. 10. These differ from the design

Table 3. Effect of severe thermal transients on the leaktightness of brazed end seals on 1.60-mm-diam triaxial cables

Cable	Helium leak rate (cm^3/s) after number of quenches shown					
	0[a]	5	10	15	25	50
	Quenched from 500°C air into 80°C water, transient >300°C/s					
1	2.7×10^{-10}	1.1×10^{-8}	7.0×10^{-9}	7.2×10^{-9}	3.6×10^{-8}	
2	7.8×10^{-10}	1.0×10^{-10}	9.7×10^{-9}	3.6×10^{-9}	2.4×10^{-8}	
3	7.8×10^{-10}	1.2×10^{-9}	2.5×10^{-9}	2.6×10^{-8}	9.6×10^{-9}	
4	5.4×10^{-9}	2.6×10^{-10}	3.2×10^{-9}	3.2×10^{-9}	2.4×10^{-8}[b]	
5	4.2×10^{-9}	4.7×10^{-9}	8.6×10^{-9}	8.0×10^{-9}	8.1×10^{-9}[b]	
	Quenched from 300°C helium by water spray, transient >200°C/s					
6	2.3×10^{-10}					4.9×10^{-6}
7	6.0×10^{-6}					6.6×10^{-6}

[a] As brazed.

[b] After 20 quenches.

Y-185784

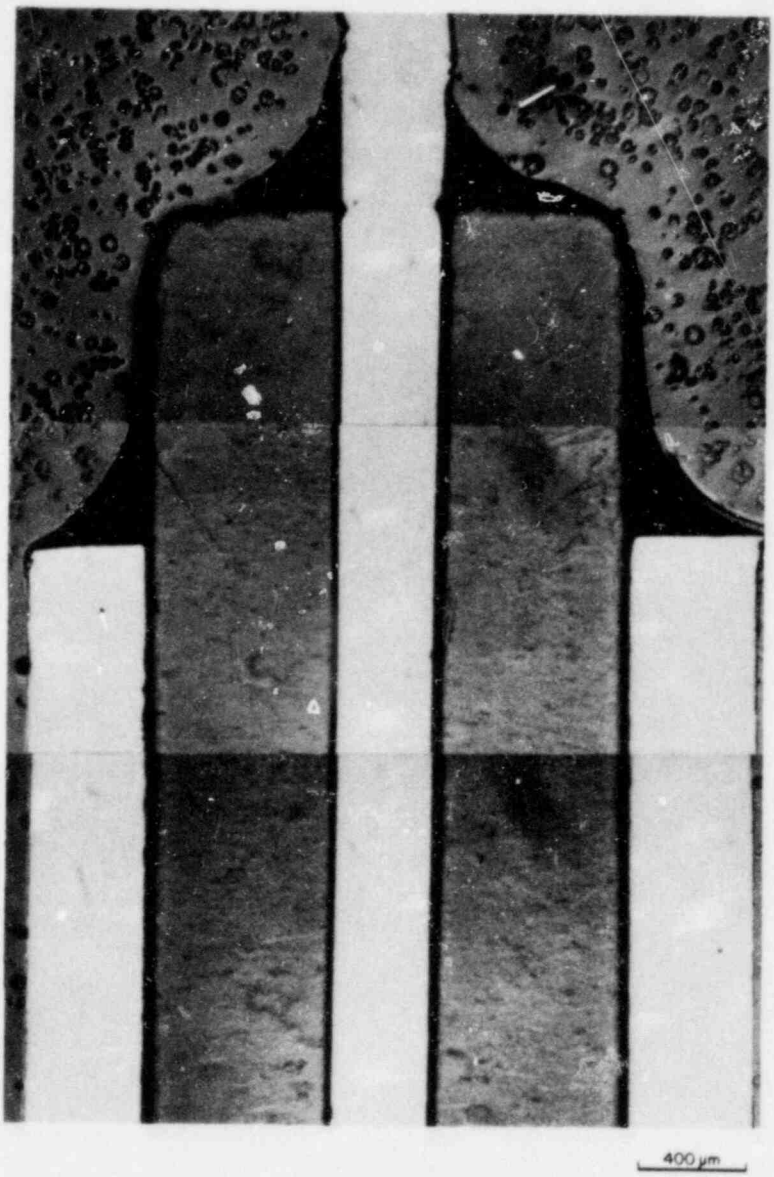

Fig. 8. Cross section of brazed ceramic-to-metal cable end seal after 25 severe thermal transients. Note that, although some cracking has occurred, there has been no gross degradation of the platinum-dispersion-enhanced ceramic insulator.

for SCTF in that the PKL body diameter is 24.76 mm (0.975 in.) versus 20.78 mm (0.818 in.) in the SCTF design. The end cap shown is also of an older design. Note that the cermet insulator in this probe is 12.7 mm (0.500 in.), which is much larger than those in our earlier work. The design of the ceramic-to-metal seal provides that the cermet be brazed to the platinum transition ring only and not to the stainless steel body. Platinum posts are brazed through the insulator for

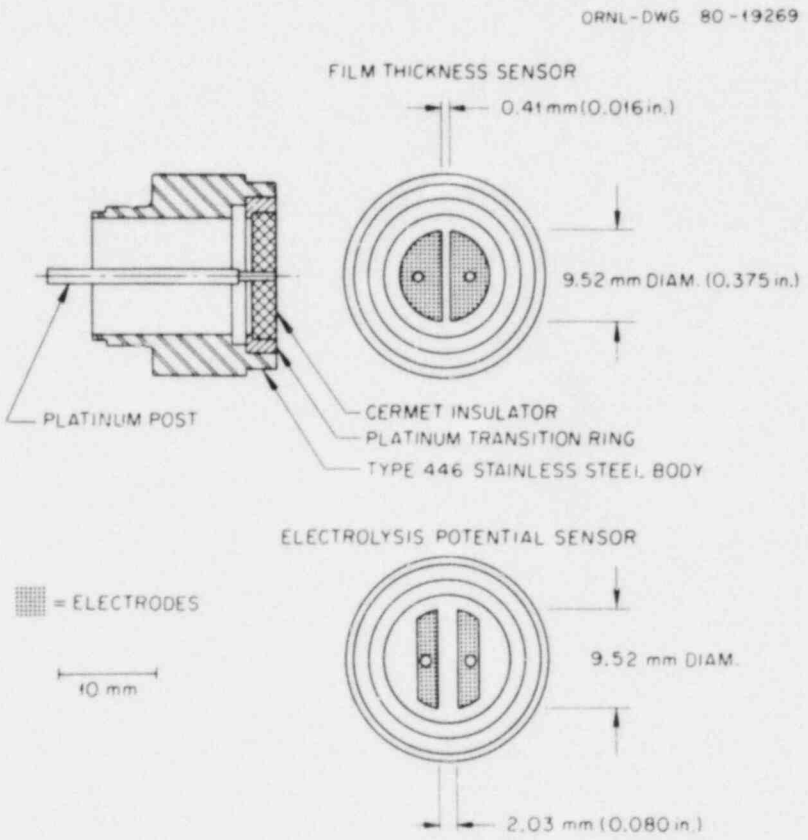

Fig. 9. Design of two types of Slab Core Test Facility-I in-wall and upper-plenum film sensor subassemblies.

connecting the central leads of the two triaxial cables to the sensor electrodes. All these subassemblies have been vacuum furnace brazed with 49% Ti–49% Cu–2% Be filler metal for 5 min @ 970°C.

In the first series of film sensors, the electrodes themselves consisted of a thin layer of brazing filler metal on the surface of the cermet. Filler metal powder was preplaced on the outside of the cermet only. After brazing, irregularities on the face of the sensor were removed with 320-grit emery paper, and the electrode pattern was produced by selective removal of the alloy down to the insulator by use of ultrasonic machining. This process uses a sonotrode (sonic electrode) in the shape of the material to be removed. The braze-coated surface of the cermet is abraded as the sonotrode is rapidly vibrated while in an abrasive slurry and in close proximity to the workpiece. Eventually all the brazing alloy is removed except for two areas in the shape of the electrodes. The more widely available electrical discharge machining (EDM) could not be used in this application because the cermet insulator precludes the required conductive path. Attempts to use EDM failed when the filler metal was not removed evenly, leaving electrically isolated islands of alloy on the surface. A sensor subassembly from this series is shown in Fig. 11.

Y-163491

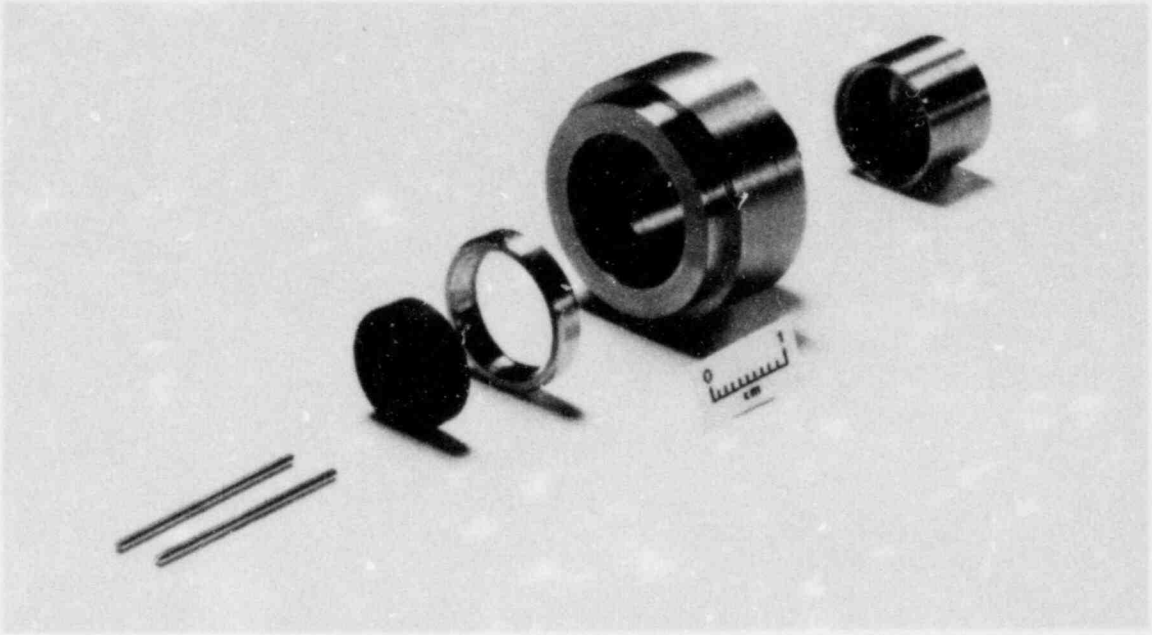

Fig. 10. Components for Primärkreislauf in-wall film probe subassembly. From left: platinum posts, cermet insulator, platinum transition ring, type 446 stainless steel body, and end cap.

This sensor model was reasonably successful, considering that it was the first of the in-wall film probe type. For example, of 25 sensor bodies of this style brazed, 5 had helium leak rates that saturated the leak detector and were rebrazed, 1 leaked at 1.2×10^{-5} cm^3/s, 16 had leak rates averaging 3.2×10^{-6} cm^3/s, and 3 had leak rates averaging 3.5×10^{-8} cm^3/s. The alloy had been placed on the face of the sensor only, and care was taken in the brazing cycle to avoid shorting out the sensor internally by alloy flow-through around the platinum posts. This prototype was also relatively resistant to thermal shock. Two samples were repeatedly quenched from 500°C into hot water and periodically tested for leakage by pressurizing internally with 0.14 MPa, gage (20 psig) He and immersing in alcohol. One subassembly had only one slow leak (about one bubble per second) after 20 cycles, and the other had a gradually increasing bubble formation rate from the 12th cycle onward.

Two areas of concern remained, however, after conducting leaktightness, thermal shock, and actual sensor tests in a steam-water system: (1) the leak rate of the subassembly and (2) the degree of flatness of the electrode face. The as-brazed leak rates per se of the series were not a major concern. However, we desired to begin with a significantly lower leak rate so that the sensors would still have adequate leaktightness after a number of reflood tests. The flatness of the electrode face is significant because any perturbations in that area limit the ability of the sensor to respond to thin films. We had tried to hold

ORNL-PHOTO 5458-80

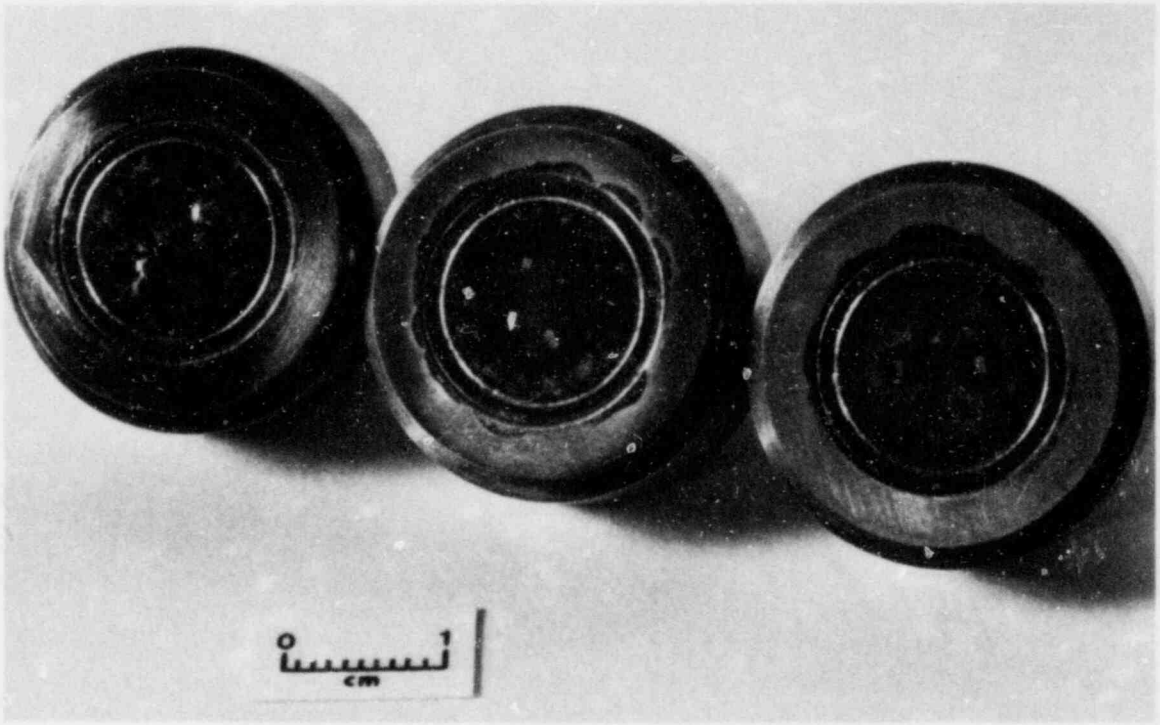

Fig. 11. Steps in fabrication of film sensor having 49% Ti–49% Cu–2% Be brazing filler metal electrodes outlined by ultrasonically machined impression. Left, as brazed. Center, after surface is sanded smooth. Right, after filler metal has been removed leaving two *D*-shaped electrodes.

the depth of the ultrasonically machined pattern outlining the electrodes to 0.02 to 0.05 mm (0.001–0.002 in.) to minimize the effect on the films passing over the surface but found that, even with great care, the depth of cut in the first series averaged 0.15 to 0.20 mm (0.006–0.008 in.). We therefore considered modifications to the design and fabrication techniques to alleviate these concerns.

Two changes made in the next series of prototypes greatly improved both the short- and long-term performance of the film probe sensor. First, the machining sequence was reversed. The Cavitron was used to abrade two shallow impressions (the shape of the electrodes) in the cermet before brazing. The electrodes had previously been outlined after brazing. In the second series, the surface of the sensor face was sanded on a metallographic wheel with 320-grit paper to remove excess filler metal down to the insulator. This step leaves only the filler metal in the electrode impressions. This change in procedure was beneficial not only because it resulted in a very smooth electrode face with no perturbations but also because the depth of cut (in the electrode cavity) was not as critical so that machining was much simpler.

The second change, which was in subassembly design, although simple in nature, is considered to be the most significant change from the

standpoint of leaktightness and thus long-term survivability of the film property sensors. The change consisted of drilling a 0.41-mm-diam by 2.54-mm-deep (0.016 by 0.100 in.) axial hole in one end of the 1.02-mm-diam (0.040-in.) platinum electrode posts that are brazed into the cermet insulator. These posts are used to connect each electrode to a triaxial cable. The purpose of the hole was to reduce the strength of the post in the area where it passes through the cermet. This minimizes the stresses that may be imposed on the braze alloy and cermet by the mismatch in thermal expansion of the components. The helium leak rates of the first three subassemblies brazed with the hollow electrode posts (and with premachined electrode cavities) indicated that this hole served its purpose. These parts had leak rates of 5.1×10^{-8}, 3.0×10^{-9}, and 2.5×10^{-9} cm^3/s. As in our earlier impedance probe work for PKL, the excess brazing filler metal bridging the gap between the electrode posts on the inside of the subassembly was removed by abrasive blasting, thereby eliminating concerns of shorting the posts out internally during brazing.

The excellent thermal shock resistance of the improved design was also evident when the third subassembly of this series was tested by dropping from air at 500°C into water at 80°C. After 10 of these severe thermal transients, the part leaked at a rate of only 8.0×10^{-7} cm^3/s, and at a rate of 2.7×10^{-7} cm^3/s after 20 cycles. The electrode surface of this prototype was subsequently polished for metallographic examination, which revealed the excellent condition of this relatively large cermet after testing, as shown in Figs. 12 and 13. Although some fine cracks occur in the insulator in the vicinity of one of the Ti-Cu-Be electrodes and the electrodes themselves contain a pattern of fine cracks and some void areas, the general appearance of the cermet is excellent. This is particularly true in light of its 20 severe thermal shock test cycles. A major concern in all our sensors is that, above all, we avoid a catastrophic failure that might release metallic debris into the process fluid. Such parts could cause major damage as the result of shorting between adjacent fuel rod simulators. We were therefore encouraged that the integrity of this sensor had been maintained during these severe tests.

The final modification to the design of the film probe subassembly was in the electrode material itself. We had realized from the beginning of our effort that the Ti-Cu-Be electrodes would gradually corrode over their lifetime in the steam-water environment. Short-term performance testing (4 h in 800°C steam, 2 h in air at 800°C, and 16 h in steam between 200 and 800°C) of a completed sensor subassembly showed that, although a light oxide film formed on the electrodes, the performance of the sensor was not impaired. However, uncertainties over the long-term effect of oxide formation and the desire to produce the best possible sensor led us to replace the Ti-Cu-Be braze alloy electrodes with inserts made of platinum as shown in Fig. 14. These electrodes were fabricated to a thickness of 0.51 mm (0.020 in.) and brazed into matching 0.38-mm-deep (0.015-in.) recesses in the cermet with the 49% Ti-49% Cu-2% Be filler metal. The electrodes are thicker than the depth of the cavities so that a small shoulder is left for preplacement of alloy.

Y-168143

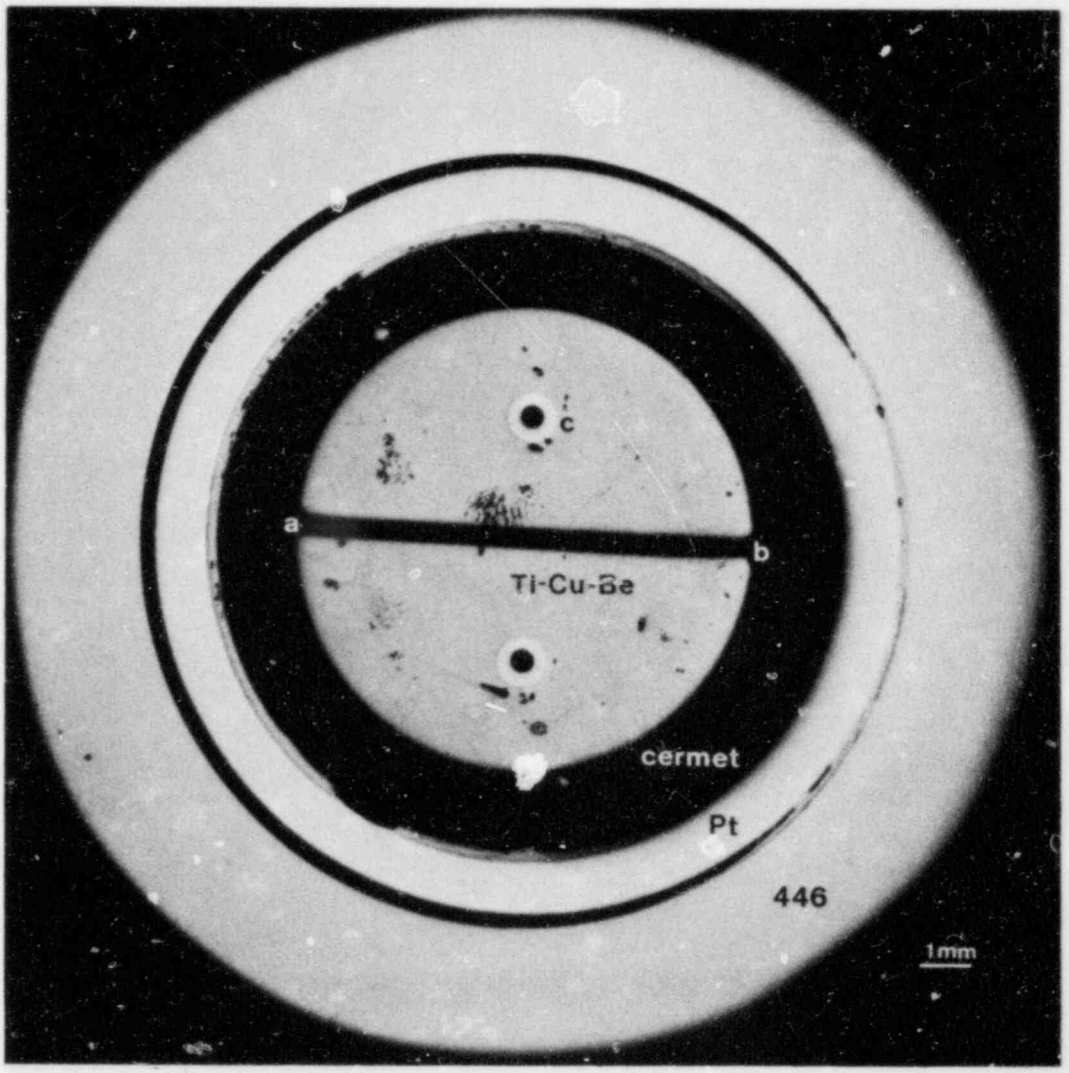

Fig. 12. Surface of in-wall film probe subassembly with 49% Ti–49% Cu–2% Be electrodes after 20 thermal shock tests from air at 500°C into water at 80°C. Selected areas (indicated by letters) are shown in greater detail in Fig. 13.

After brazing, the electrode face of the subassembly was again ground on a metallographic abrasive wheel to flatten the surface and to remove the braze alloy from the insulator. As in the previous series of sensor subassemblies, we also preplaced brazing filler metal powder around the platinum posts on the inside of the cermet for added leaktightness assurance. Some of this alloy was subsequently removed by careful grit blasting so that the posts and connecting electrodes were electrically isolated. This technique also leaves a smooth fillet of filler metal at the intersection of the post and cermet.

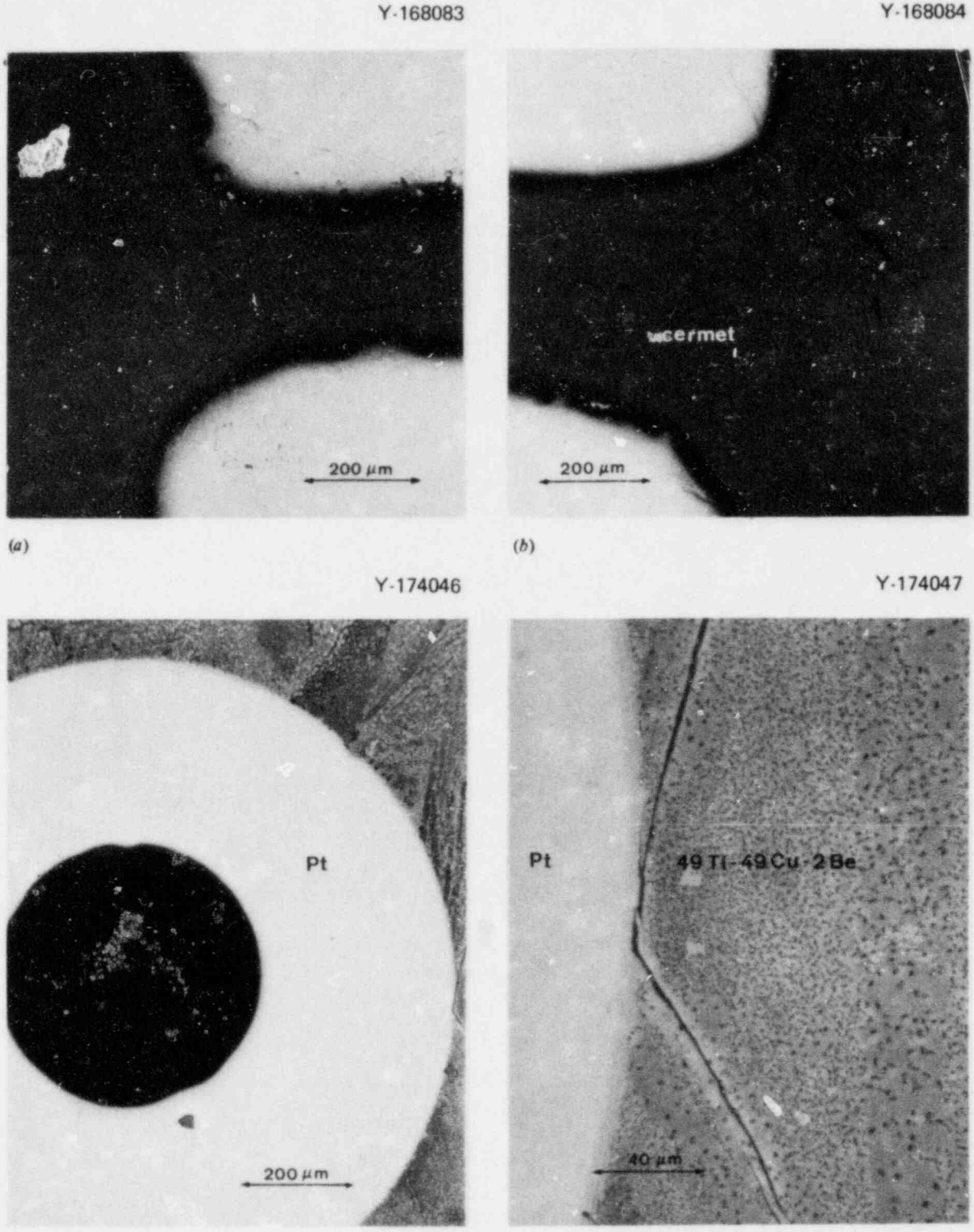

Fig. 13. Microstructure of selected areas of surface of film probe subassembly (Fig. 12) after 20 severe thermal transients. As polished.

ORNL-PHOTO 5454-80

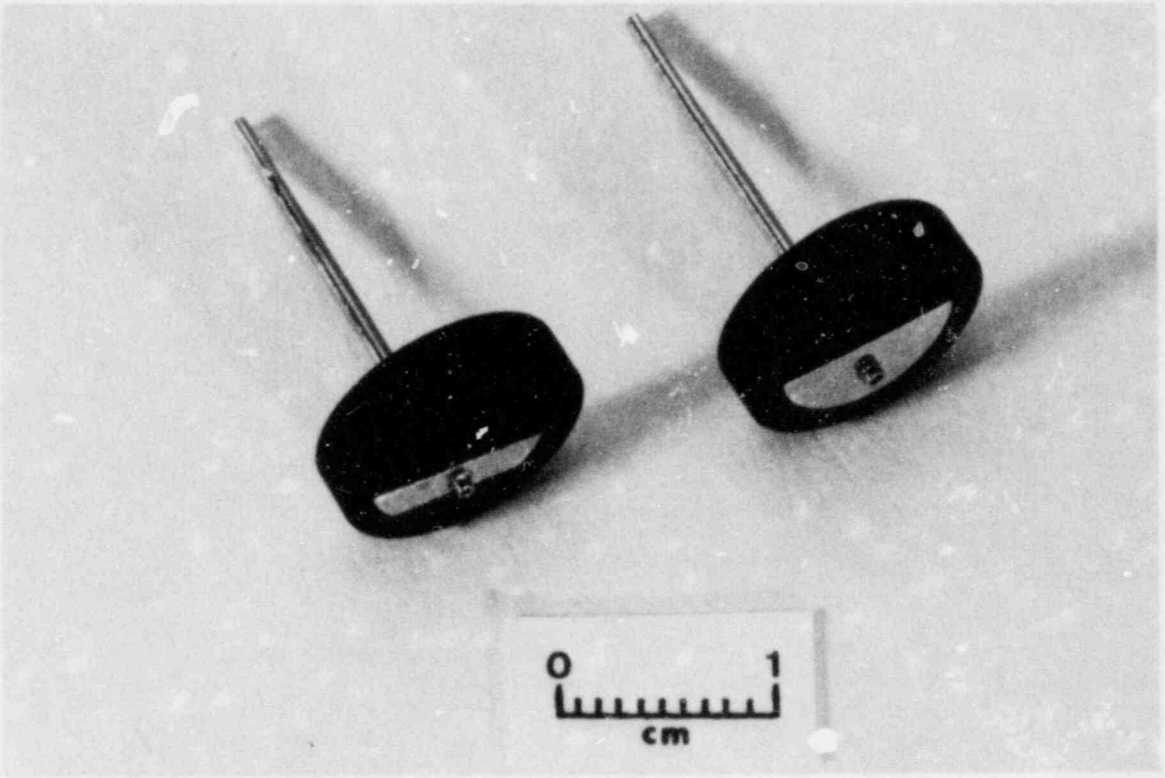

Fig. 14. Dispersed-platinum alumina insulators with platinum electrodes in depressions made by ultrasonic machining.

The as-brazed leaktightness and electrical properties of the film probe sensors with platinum electrodes was similar to the series with Ti-Cu-Be electrodes. For example, of 50 subassemblies brazed as part of a series intended for the SCTF system, only 2 were electrically shorted below the surface of the cermet and could not be used. Of the remaining 48, 6 had helium mass spectrometer leak rates greater than 9×10^{-7} cm^3/s and were rebrazed, 8 had leak rates of about 10^{-7} cm^3/s, 20 of about 10^{-8}, and 14 had leak rates of 10^{-9} or lower. The various steps in fabrication of sensor bodies in this series are illustrated in Fig. 15

THERMAL SHOCK TESTING

Representative samples of brazed film probe subassemblies with platinum electrodes were tested in a series of ten tests in which the samples were dropped from air at 330°C into water at 80°C, followed by 25 quenches from 500°C air into hot water. The severity of these tests was intended to determine the resistance of this design to thermal transients of the magnitude expected in a reflood facility. The effect

ORNL-PHOTO 4176-80

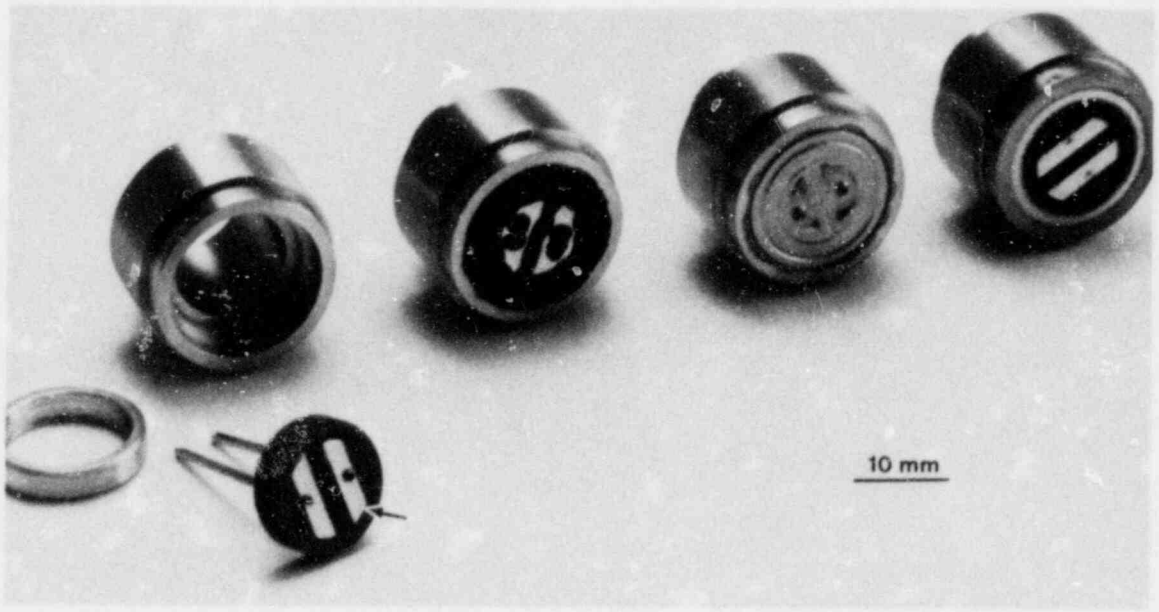

Fig. 15. Various stages of fabrication of Slab Core Test Facility-I in-wall film probe subassembly. From left: Components with platinum electrodes (arrow) in recesses in cermet, after brazing filler metal is applied, after brazing, and after grinding of sensor face.

of such thermal shock on the leaktightness of three subassemblies is given in Table 4. Note the excellent (considering the thermal history) helium leaktightness of these components after testing. The success of this series of tests resulted in our taking the film probe sensor with platinum electrodes as the reference design for both the PKL and SCTF test facilities.

BRAZING OF END CAPS

The final subassembly to be made before completion of the film probe sensors was the attachment of two triaxial cables (with brazed end seals) and a 1.60-mm-diam type 304 stainless steel vent tube into an end cap that would eventually be joined to the brazed sensor body. Our first attempt at fabricating the end cap subassembly involved vacuum furnace brazing two cable end seals, the cables themselves, and a vent tube into a short end cap (Fig. 10) in one operation. This design, although having the advantage of minimizing fabrication steps and using a shorter end cap (which is an advantage in some closely confined areas), was abandoned after development efforts proved it to be very difficult to braze, inspect, and if necessary repair. In the modified design we have avoided making all the brazes in one operation; instead, the end cap subassembly is fabricated in two steps. First, end seals are brazed

Table 4. Effect of severe thermal transients on the leaktightness of in-wall film probe sensors

Sensor[a]	Helium leak rate after number of quenches shown (cm^3/s)							
	0[b]	5[c]	10[c]	15[d]	20	25	30	35
313	1.3×10^{-5}	1.0×10^{-5}	1.2×10^{-5}	3.1×10^{-5}	1.8×10^{-5}	1.3×10^{-5}	8.0×10^{-6}	9.0×10^{-6}
315	5.5×10^{-10}	1.5×10^{-9}	1.5×10^{-9}	2.4×10^{-7}	2.2×10^{-7}	1.8×10^{-7}	1.0×10^{-7}	2.0×10^{-7}
402	2.0×10^{-6}	2.8×10^{-7}	2.4×10^{-6}	5.5×10^{-6}	1.2×10^{-5}	1.2×10^{-5}	7.5×10^{-6}	3.8×10^{-6}

[a] Al_2O_3-Pt cermet insulator (12.7 mm diam × 2.5 mm thick).

[b] As brazed.

[c] Dropped from air at 330°C into water at 80°C.

[d] Air at 500°C into water at 80°C.

on individual cables (as previously discussed) with Ti-Cu-Be filler metal. After the cables have passed the leak and electrical checks, they are induction brazed, along with a vent tube, into a longer type 446 stainless steel end cap (Fig. 16). This technique ensures that only acceptable cables are brazed into subassemblies and allows us to concentrate on brazing the cables into the end cap without being concerned with making the difficult end seal brazements. Leak checking the cables is also greatly simplified, and leaking cables can be identified and rebrazed if necessary. As shown in Fig. 16, the induction brazing operation is carried out with the end cap in a vertical position, supported on a quartz pedestal. A small glass chamber maintains an argon atmosphere around the heated area. By brazing in the vertical

ORNL-PHOTO 4150-80

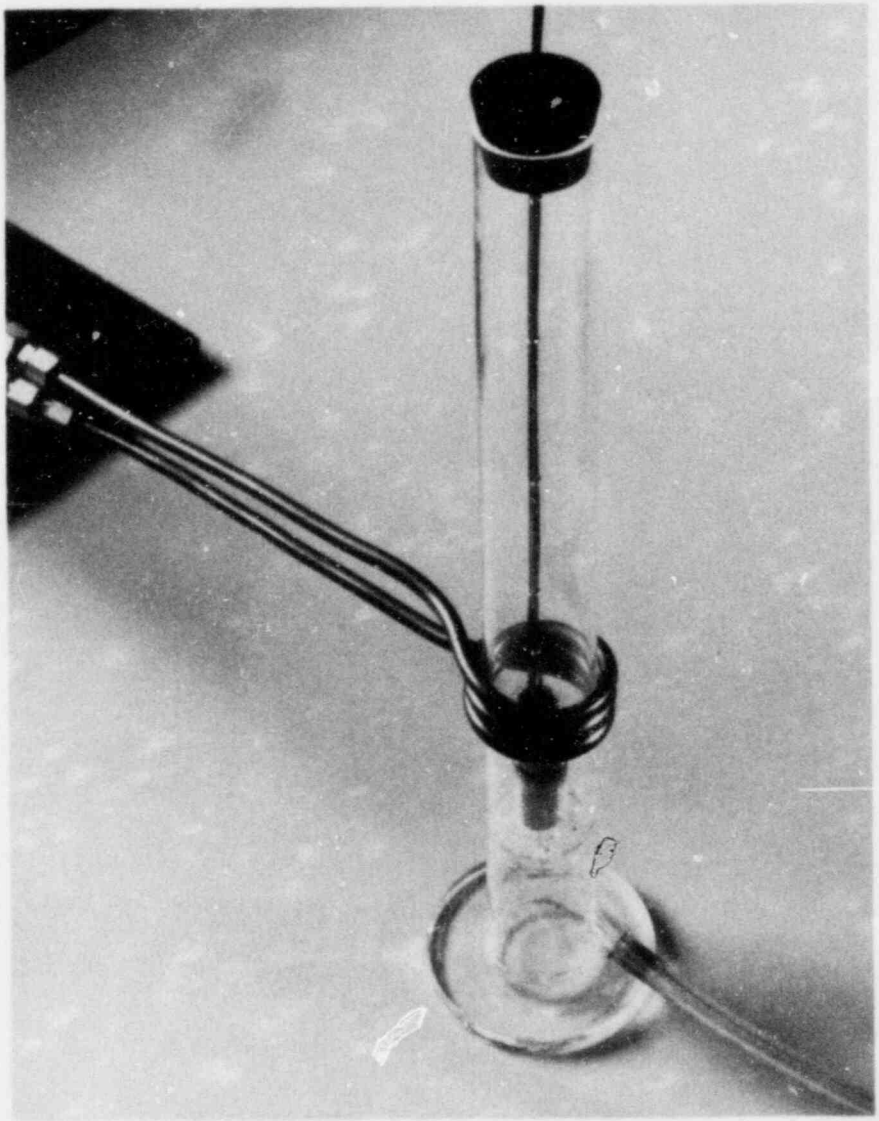

Fig. 16. Induction brazing two triaxial cables and a vent tube into a type 446 stainless steel end cap.

position we can ensure that the commercial BNi-2 (Ni-7% Cr-4% Si-3% Fe-3% B) brazing filler metal powder is kept in the joint area before and after melting. This alloy was chosen because we had found it to have excellent steam corrosion resistance and minimal erosion tendencies on stainless steel and to be less susceptible to displacement by the induction field than some other nickel-base filler metals. Brazing is by manual control of the induction power supply with the operator visually determining when flow is adequate. One of the 13.7-mm-diam by 38.1-mm-long (0.540 by 1.500 in.) type 446 stainless steel end caps is shown after brazing in Fig. 17. The end cap is long enough that there is only minimal heating of the triaxial cables in the end seal area. The area over which the cables are brazed to the end cap and the degree of coupling with the radiofrequency waves from the induction coil are enhanced by having a 14.5-mm-thick (0.57-in.) solid section on the end of the cap.

ORNL-PHOTO 5455-80

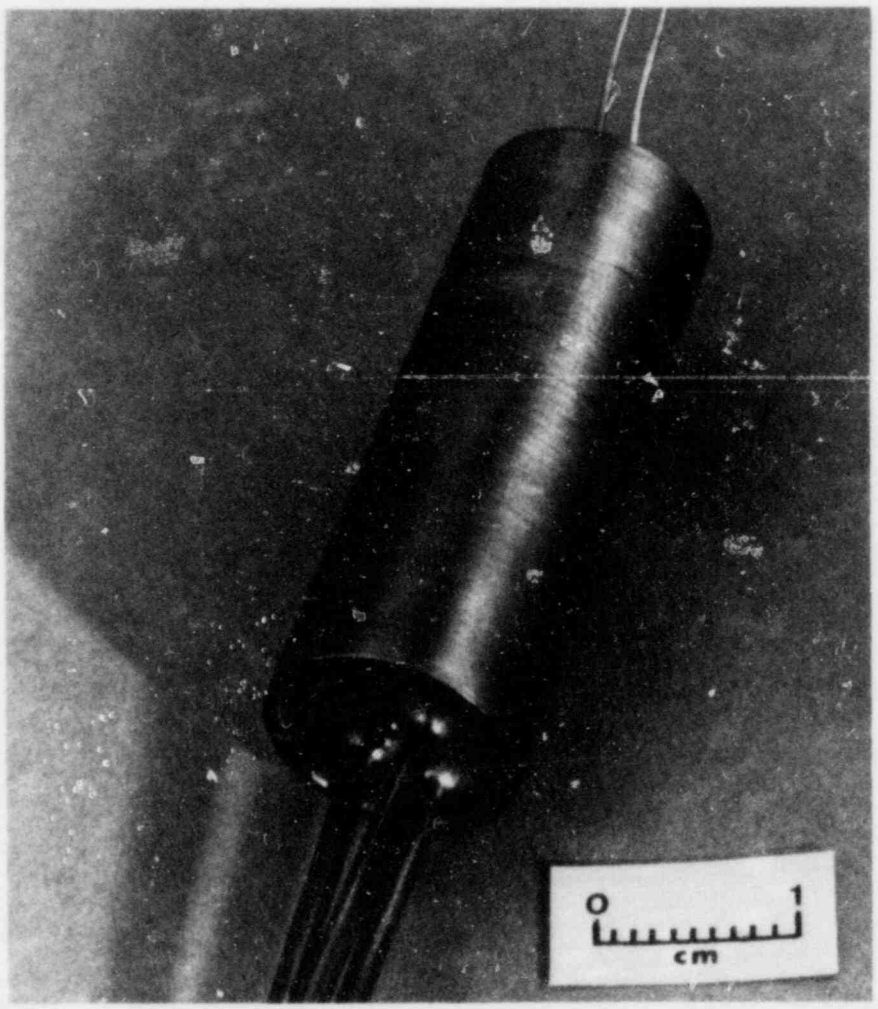

Fig. 17. Type 446 stainless steel end cap induction brazed to two triaxial cables (with brazed end seals) and a type 304 stainless steel vent tube. The brazing filler metal composition was Ni-7% Cr-4% Si-3% Fe-3% B.

FILM PROBE SENSOR ASSEMBLY

After final measurement of the helium leak rate and electrical properties of the two subassemblies, these components are joined by a circumferential pulsed laser weld to form a sensor assembly. Sapphire bead insulators are threaded onto the platinum extension wires (Fig. 18) of the two coaxial cables before laser welding the wires to the posts of the sensor subassembly body and making the closure weld. (A small vacuum probe greatly reduces the difficulty of threading the beads onto the wire; the beads are necessary to prevent the cable extension wires from coming in contact with each other or the probe wall in the close confines of the sensor body.) The spherical geometry of the insulators was chosen because it allows flexible movement of the platinum leads as they are bent in a "Z-fold" configuration to allow movement of the end cap into place (Fig. 19) without breaking the laser weld joining the leads to the platinum posts.

A step joint is used between the sensor body and end cap because that configuration is self-aligning and a full-penetration weld is not

ORNL-PHOTO 4151-80

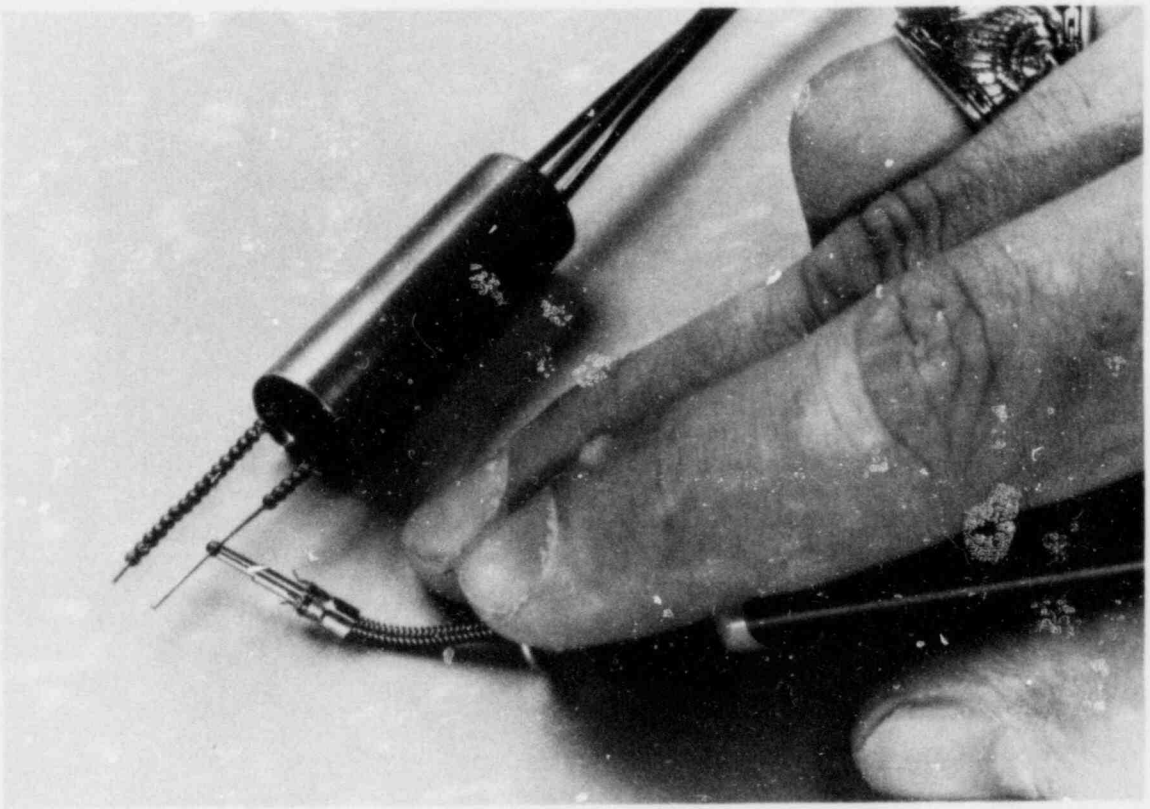

Fig. 18. Installation of 1.60-mm-diam (0.063-in.) sapphire bead insulators on platinum leads extending from the triaxial cables before laser welding the end cap to the sensor subassembly.

ORNL-PHOTO 4149-80

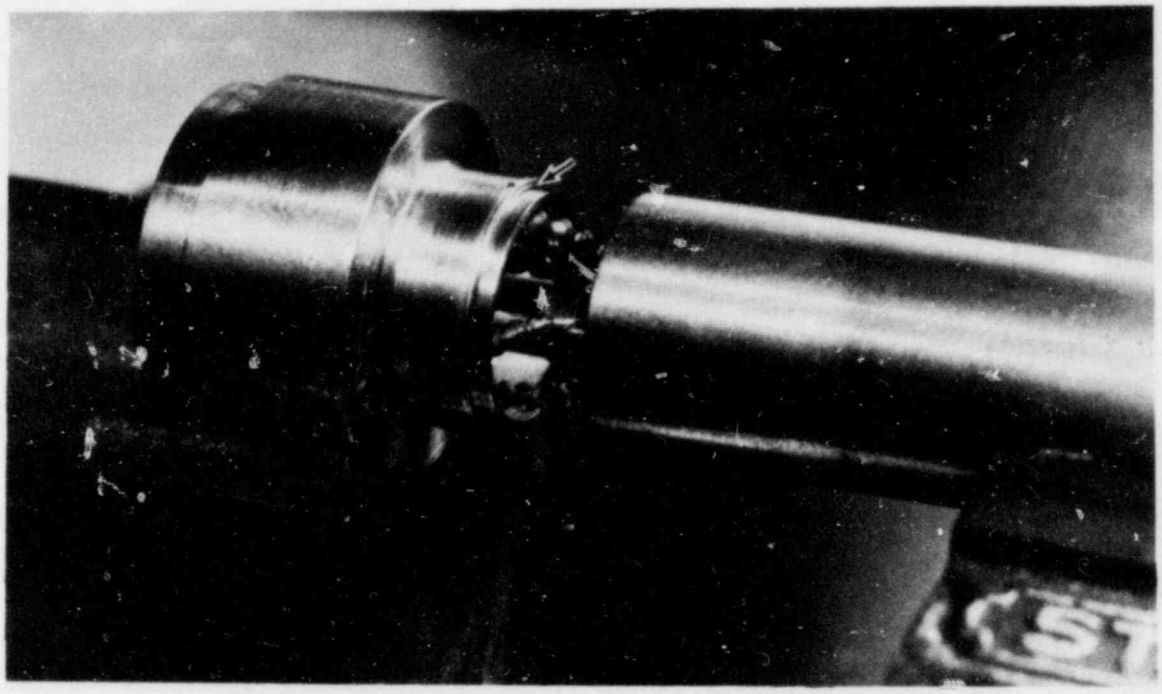

Fig. 19. Mating of sensor subassembly (left) and end cap before joining by laser welding. Two strands of 0.25-mm-diam (0.010-in.) filler wire were laser tack-welded to the sensor subassembly in the step joint area (arrow).

required. This design also provides support for two strands of small-diameter filler wire that are tack-welded to the body before welding (Fig. 19) and eliminates concern that the laser beam passing through a gap in the joint (as it might in a butt joint) might damage the fine leads underneath.

Although a number of film probe assemblies were successfully fabricated with a low-power (<10 J per pulse) ruby laser welder, we are currently using only the high-power pulsed Nd:YAG laser shown in Fig. 20. This unit produces a significantly deeper penetration weld at a much higher welding speed.

The first efforts at laser welding the type 446 stainless steel end cap and sensor body resulted in welds that looked good visually but that, on metallographic examination, were unacceptable because of a number of fine cracks [Fig. 21(*a*)]. These welds were made with the following parameters: (1) 3-ms pulse length, (2) 40 pulses per second, (3) sharp focus, (4) 8 s per revolution part rotation, (5) 10-s welding time, and (6) argon shielding gas. The laser beam power was about 170 W. Two strands of 0.25-mm-diam (0.010-in.) type 308 stainless steel filler were used; note that full penetration of the 0.50-mm-thick (0.020-in.) step was achieved.

By comparing the cross-sectional area of the filler wire with the area of the weld fusion zone (counting squares in a grid superimposed

ORNL-PHOTO 4152-80

ORNL-PHOTO 4145-80

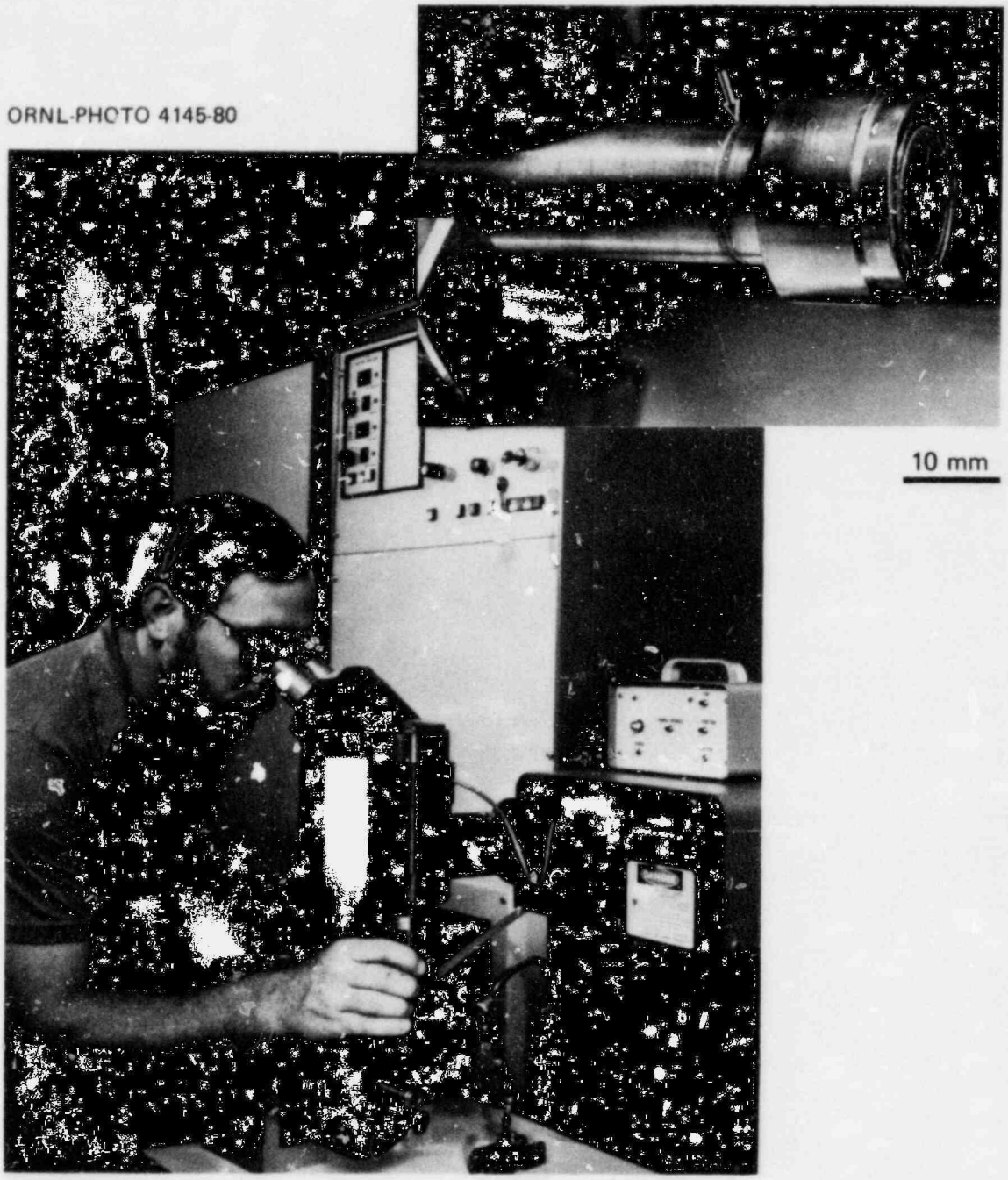

Fig. 20. Joining end-cap subassembly to brazed sensor body with high-power high-pulse-rate Nd:YAG laser welder. The weld bead is indicated by an arrow in the inset photo.

Y-177681

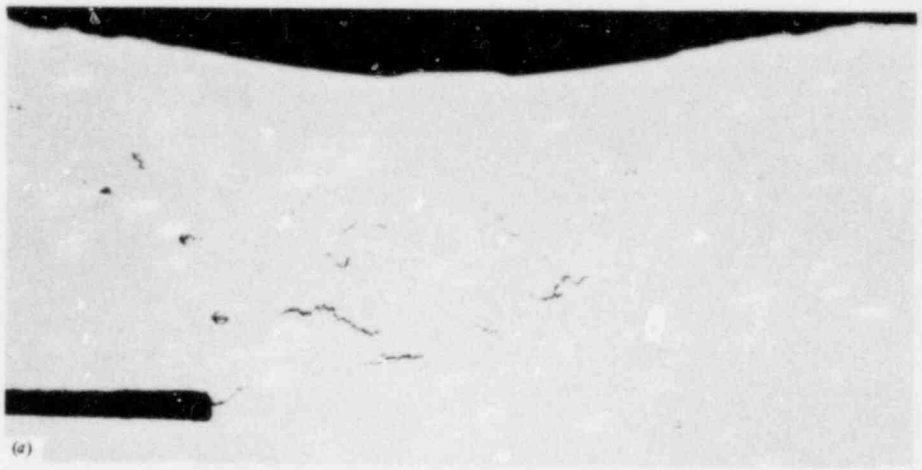

Y-177683

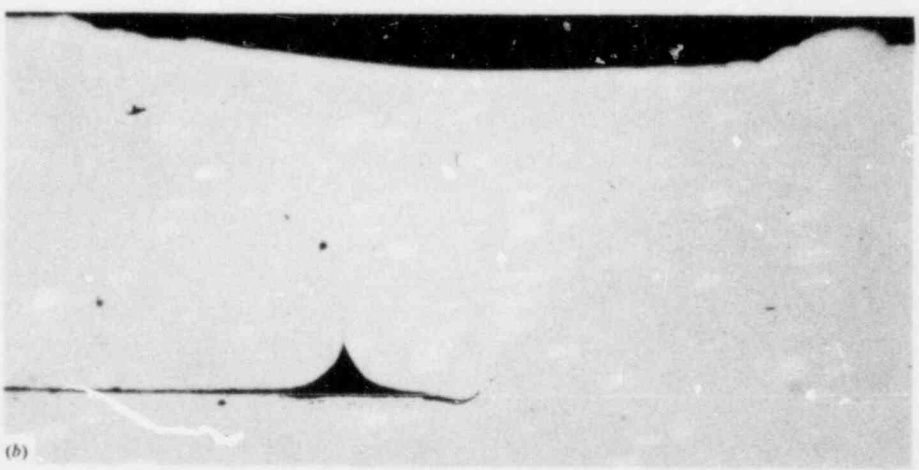

Y-177678

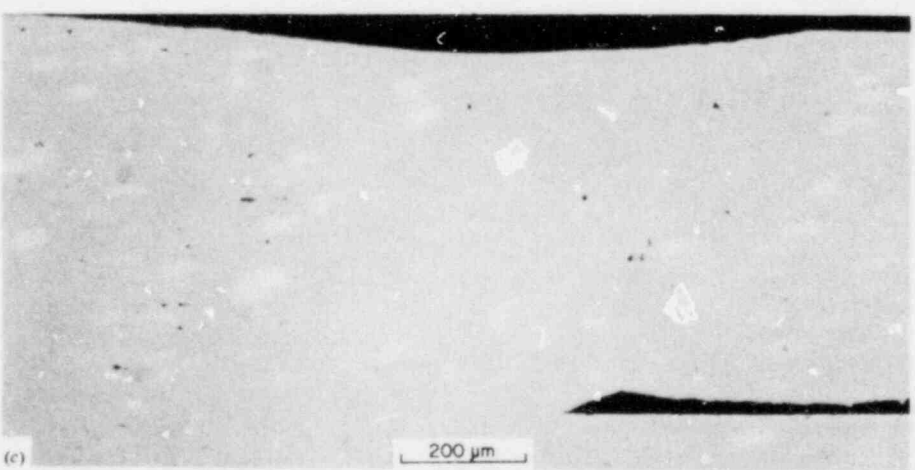

Fig. 21. Sequence of development of laser weld joining type 446 stainless steel end cap and sensor body. (*a*) Type 308 stainless steel filler, 170 W. (*b*) Type 308 stainless steel, 120 W. (*c*) Type 310 stainless steel, 140 W.

on a photomicrograph), we determined that the weld had about 80% dilution (i.e., the weld consisted of about 80% type 446 and 20% type 308 stainless steel). Using this information and a DeLong diagram[5] that relates weld metal composition to a predicted level of δ-ferrite, we could estimate that the weld would contain very high levels of δ-ferrite, which in this case was apparently contributing to weld cracking. We concluded that we could improve the weld by minimizing the volume of type 446 stainless that was melted and thereby reduce weld metal dilution. This was accomplished by reducing the laser beam power to 120 W and holding all other parameters constant. Figure 21(*b*) shows that the objective of eliminating weld cracking was almost achieved but that the weld had not quite reached full penetration. Full penetration was achieved (with similar minimal cracking) with 140-W beam power, and this value was subsequently used in welding a large number of assemblies for the SCTF.

The pressures of limited developmental funds and impending production needs forced us to make an engineering decision to use type 308 stainless steel filler and 140-W beam power for this weld, although it was evident that there was still likelihood of a small amount of fusion zone cracking. Our decision was made with the assumption that these fine cracks would not propagate during the short life of a sensor; in retrospect, this was a good decision. To date a large number of these sensor subassemblies have survived over 25 severe thermal transients with no evidence of weld failure. We have had some anomalous instances of cracking in the weld heat-affected zone, but this is apparently related to a much longer than expected immersion in water having a relatively high chloride ion content.

We have recently evaluated the use of type 310 stainless steel filler wire. Using this material would be expected to reduce δ-ferrite levels to those more typically found in austenitic stainless steel weldments. As shown in Fig. 21(*c*), the goal of producing crack-free welds was achieved.

One of the end products of this development effort is shown in Fig. 22. As shown, three of the film thickness sensors and an electrolysis potential sensor were mechanically fastened in an assembly to be installed in the SCTF-I system in either the core wall or upper plenum region. A sheath-type thermocouple is shown in the center of the array.

SUMMARY

We developed pulsed laser welding and brazing techniques for fabrication of complex sensors for measurement of film thickness and velocity during LOCA tests in simulated pressurized-water nuclear reactors. The outstanding capability of these sensors to survive repeated exposure to high-temperature steam and water and severe thermal transients was made possible by a unique ceramic-to-metal seal system. This seal is based on a metal-dispersion-enhanced ceramic insulator and an experimental brazing filler metal, both developed at ORNL.

ORNL-PHOTO 4178-80

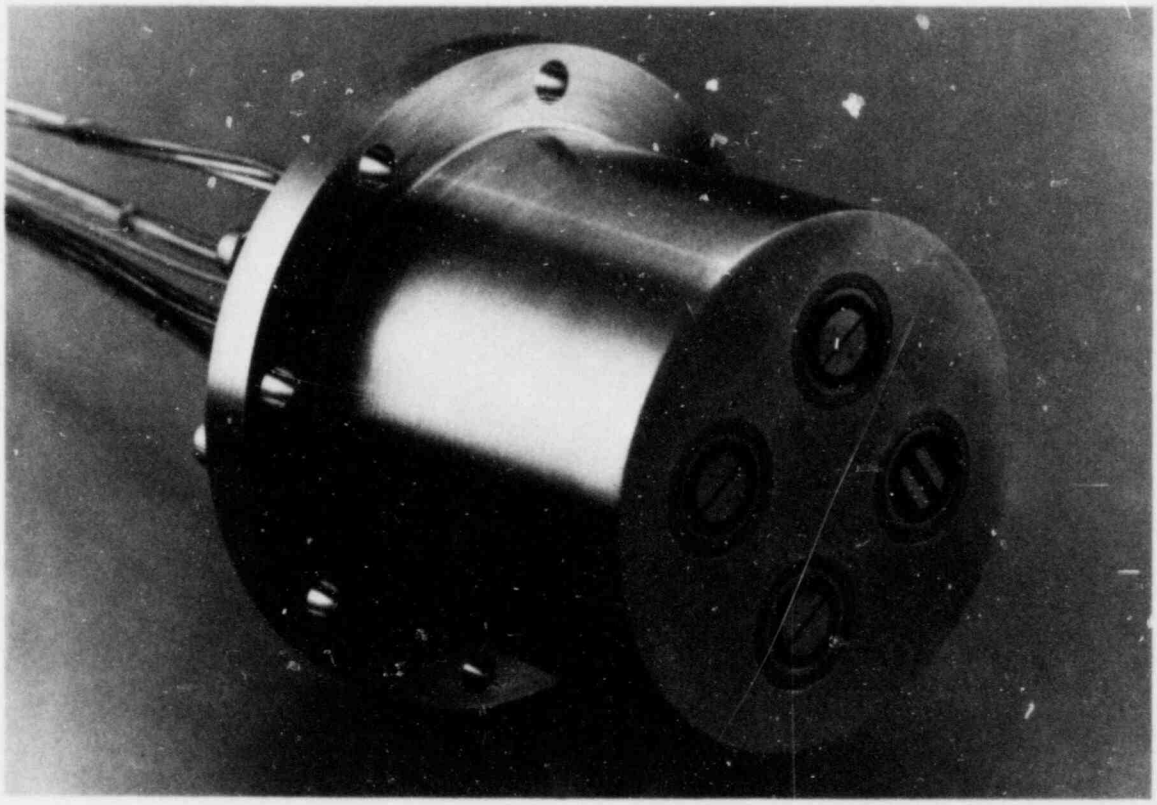

Fig. 22. Slab Core Test Facility-I wall and upper plenum film probe assembly. Cylinder portion in foreground is 76 mm in diameter.

Each of the sensor electrodes is connected to its monitoring instrument by a 1.60-mm-diam (0.063-in.) triaxial stainless steel cable, which is terminated on the process fluid end by a small-diameter ceramic-to-metal seal. The ceramic insulator in each end seal is connected to the outer sheath of the conductor and to a central lead wire by a furnace brazing process and our 49% Ti-49% Cu-2% Be filler metal. This braze alloy wets the components without the normally needed metal plating on the ceramic. These end seals routinely have excellent electrical properties (high resistance, low loss) and helium leaktightness after brazing. More significantly, prototypes subjected to repetitive thermal transients (>300°C/s) had helium leak rates of less than 1×10^{-7} cm^3/s after 25 tests.

The film sensor bodies themselves consist of a type 446 stainless steel housing that holds a relatively large platinum-dispersion-enhanced ceramic insulator (12.7-mm diam), flush-mounted platinum electrodes, and platinum posts for connection of the triaxial cables to the electrodes. The subassemblies are fabricated by furnace brazing with the Ti-Cu-Be filler metal and typically have as-brazed helium leak rates of less than 10^{-7} cm^3/s. Prototypes of these sensors were evaluated for resistance to thermal shock and were found to leak at rates of 10^{-6} cm^3/s or less after 35 severe transients.

A number of other joining techniques were also developed for fabrication of these complex sensor assemblies. For example, pulsed laser welding was used to join the sensor bodies to an end cap subassembly. The latter is produced by an induction heating operation in which two small-diameter cables and a vent tube are brazed into a cylindrical cap with a commercial nickel-base filler metal. As a result of these developments, hundreds of film property sensors were fabricated and installed in the SCTF in Japan. To date they have been succesful in surviving 25 test cycles, which is half their design life.

ACKNOWLEDGMENTS

The author would like to express his appreciation to the following individuals, who made significant contributions to this work: D. O. Doyle, T. D. Owings, R. W. Reed, and J. J. Woodhouse were responsible for the development of welding and brazing techniques. R. E. McDonald supervised the machining of all components at Thermo Electron Corporation, Woburn, Massachusetts, under the direction of E. V. Anderson and W. Baker. Cavitron machining of electrode cavities was also performed at ORNL, with R. L. Clark supervising. The metallography was by C. P. Haltom, and the photography was by L. R. McCrary. A special thanks is extended to D. B. Lloyd, who had overall responsibility for fabrication of the production lot of sensors. The manuscript was reviewed by D. B. Lloyd and J. O. Stiegler, edited by Irene Brogden, and postedited by Sigfred Peterson.

REFERENCES

1. A. J. Moorhead et al., *Fabrication of Sensors for High-Temperature Steam Instrumentation Systems*, ORNL/NUREG-65, May 1980.

2. J. C. Chen et al., "Development of Instrumentation for the Measurement of Thickness and Velocity of Thin Water Films," paper presented at the 6th Water Reactor Safety Research Information Meeting, Washington, D.C., Nov. 6-9, 1978.

3. C. Britton, R. A. Hess, and C. J. Remenyik, *Development of Film Thickness and Velocity Sensors for High-Temperature Steam-Water Systems*, ORNL report in preparation.

4. Taylor Lyman, ed., *Metals Handbook, Properties and Selection of Metals*, 8th ed., vol. 1, American Society for Metals, Metals Park, Ohio, 1961.

5. C. J. Long and W. R. DeLong, "The Ferrite Content of Austenitic Stainless Steel Weld Metal," *Weld. J. (Miami)* 52(7), 281-s-97-s (1973).

NUREG/CR-2811
ORNL-5895
Distribution
Category R5

INTERNAL DISTRIBUTION

1–2. Central Research Library
3. Document Reference Section
4–5. Laboratory Records Department
6. Laboratory Records, ORNL RC
7. ORNL Patent Section
8. P. F. Becher
9. R. G. Berggren
10. R. A. Bradley
11. R. H. Bryan
12–14. F. R. Cox
15. B. G. Eads
16. W. Fulkerson
17. U. Gat
18. M. B. Herskovitz
19. F. O. Hoffman
20. H. W. Hoffman
21. T. S. Kress
22. R. J. Lauf
23. C. G. Lawson
24. A. L. Lotts
25–29. A. J. Moorhead
30. A. C. Schaffhauser
31. G. M. Slaughter
32. K. H. Valentine
33. R. C. Ward
34. F. W. Wiffen
35. Alan Lawley (Consultant)
36. T. B. Massalski (Consultant)
37. R. H. Redwine (Consultant)
38. K. M. Zwilsky (Consultant)

EXTERNAL DISTRIBUTION

39. NRC, OFFICE OF NUCLEAR REGULATORY RESEARCH, Washington, DC 20555
Program Sponsor

40. DOE, OAK RIDGE OPERATIONS, OFFICE, P.O. Box E, Oak Ridge, TN 37830
Office of Assistant Manager for Energy Research and Development

41–42. DOE, TECHNICAL INFORMATION CENTER, P.O. Box 62, Oak Ridge, TN 37830

43–427. For Distribution Category R5 (10 – NTIS)

☆U.S. GOVERNMENT PRINTING OFFICE: 1982-546-067/162